2010

Interlaminate strength of laminated die tooling

Jenna Faith Pritchard
Iowa State University

Interlaminate strength of laminated die tooling

by

Jenna Faith Pritchard

A thesis submitted to the graduate faculty

in partial fulfillment of the requirements for the degree of

MASTER OF SCIENCE

Major: Industrial Engineering

Program of Study Committee:
Frank E. Peters, Major Professor
Matthew C. Frank
Palaniappa A. Molian

Iowa State University

Ames, Iowa

2010

Table of Contents

List of Figures

List of Tables

Acknowledgements

I would like to thank my major professor, Dr. Frank Peters for his encouragement throughout my time at Iowa State University. His support and guidance helped throughout this research project. I would also like to thank my committee members, Dr. Matthew Frank and Dr. Palaniappa Molian for their time and support throughout my graduate career. Lastly, I would like to thank my friends and family for their support during my time at Iowa State University.

Abstract

This thesis examines process planning for rapid die tooling. Sheet metal die tooling typically requires long lead times from design to manufacturing. Rapid manufacturing of die tooling is a method that reduces lead times by minimizing the process planning time. This research focuses on the process planning algorithm for laminated die manufacture to automatically provide adequate interlaminate strength using a minimum number of fasteners.

A mechanical model was developed for predicting shear and compressive forces during sheet metal bending was developed as an input to a bolt and dowel pin algorithm. An algorithm is described for proper placement of bolts and dowel pins per each slice layer to satisfy the mechanical model. The impact of this research will allow for proper design to achieve mechanical requirements of die tooling in a rapid manufacturing technology.

Chapter 1. Introduction

Sheet Metal Forming Overview

Sheet metal products are important in a variety of industries, including automotive and aerospace. Components formed from sheet metal can be strong, lightweight, and quite inexpensive in large volumes. Furthermore, it is relatively simple to achieve complex surface geometries without increasing processing costs.

Sheet metal is considered to have thicknesses between 0.4 mm (1/64 in.) and 6 mm (1/4 in.) (Groover, 2002). Sheet metal rolls are typically produced by hot or cold rolling. Geometry created from sheet metal rolls (both in-plane and out-of-plane) can be generated through a number of processes: punching, bending, and drawing.

Punching is an operation where in-plane geometry is created by selective removal, Figure 1. The primary mechanism of punching is *shearing*, where the perimeter of the metal undergoes extremely high stresses until it yields and separates.

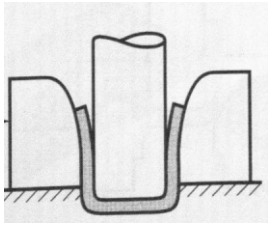

Figure 1. Punching operation (Groover, 2002)

Drawing is a common sheet metal operation for applications such as beverage cans, ammunition shells, sinks, cooking pots, and automobile body panels (Groover, 2002). The sheet metal is placed over a die. A punch pushes the sheet metal into the die to form the desired geometry. The mechanisms of plastic deformation are both bending and stretching, though the complicated 3-dimensional nature of the process makes these modes much more difficult to model and understand than pure shearing or simple bending.

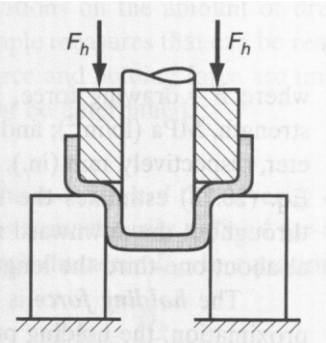

Figure 2. Deep drawing operation (Groover, 2002)

Bending deforms sheet metal around a straight axis (Groover, 2002). Bending deforms the flat sheet metal through v-bending or edge bending. The primary mechanism of bending is plastic deformation within a limited region. A common problem with bending is springback of the sheet metal due to lagging in the plastically deformed zone (Groover, 2002).

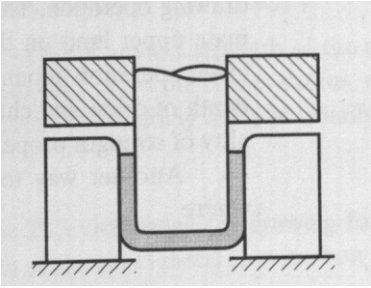

Figure 3. Bending operation (Groover, 2002)

Drawing is often the most complex of sheet metal forming. While certain regions of the sheet are stretched, compressive buckling causes wrinkling of the final product in other regions. If stretched too far, the sheet may tear due to high tensile strains from metal thinning.

Regardless of the process, sheet metal is formed by some type of die tooling. While dies are often large and expensive, their cost is amortized over a high number of final products, making them an economical way of shaping high volumes of sheet metal parts. Tool and die

materials often include steels, carbides, and ceramics (Metals, 1982) and have a high surface hardness – Rockwell C 60 or higher (Metals, 1982) – in the interests of long tool life. The die tooling is typically fabricated by machining a bulk material and post-process surface grinding. Because of the aforementioned process defects, several iterations of the die tooling may be required to obtain correct defect-free sheet metal geometry in the final product (Walczyk & Hardt, 1999).

Such as with most tooling, high cost and time is required in design and fabrication of die tooling. Die tooling failures can arise from poor designs. Sharp corners, poorly located grooves, abrupt changes in section, thin walls, and improper clearances are undesirable designs in dies that could result in poor sheet metal forming (Metals, 1982).

Rapid Manufacturing Die Tooling

Developing the correct die the first time is difficult due to the many design considerations. This makes die tooling a good candidate for rapid manufacturing. Rapid manufacturing reduces the process of manufacturing a part or tool to a fundamental means, such that the part or tool can be carried out quickly, reliably, and economically. Rapid manufacturing reduces this to a fundamental state that will repeatedly work.

Rapid manufacturing technology has evolved from three building processes: additive, subtractive, and hybrid. Traditional rapid manufacturing, which emerged in the late 1980's, built 3D models from an additive process. A 2D cross-sectional slice of the 3D model is evaluated for material deposition. Slices are built layer by layer producing an *additive* process. *Subtractive* process is used in CNC machining (or other material removal processes) where material is removed from the stock material. *Hybrid* processes use combinations of additive and subtractive processes. One type of hybrid process involves material layers placed similar to the additive process and the excess material is removed from the layer by use of tooling similar to the subtractive process. Each type of process step has its own advantages; additive process steps give extreme flexibility in geometry, while subtractive process steps can help achieve excellent tolerances and surface finishes, Figure 4.

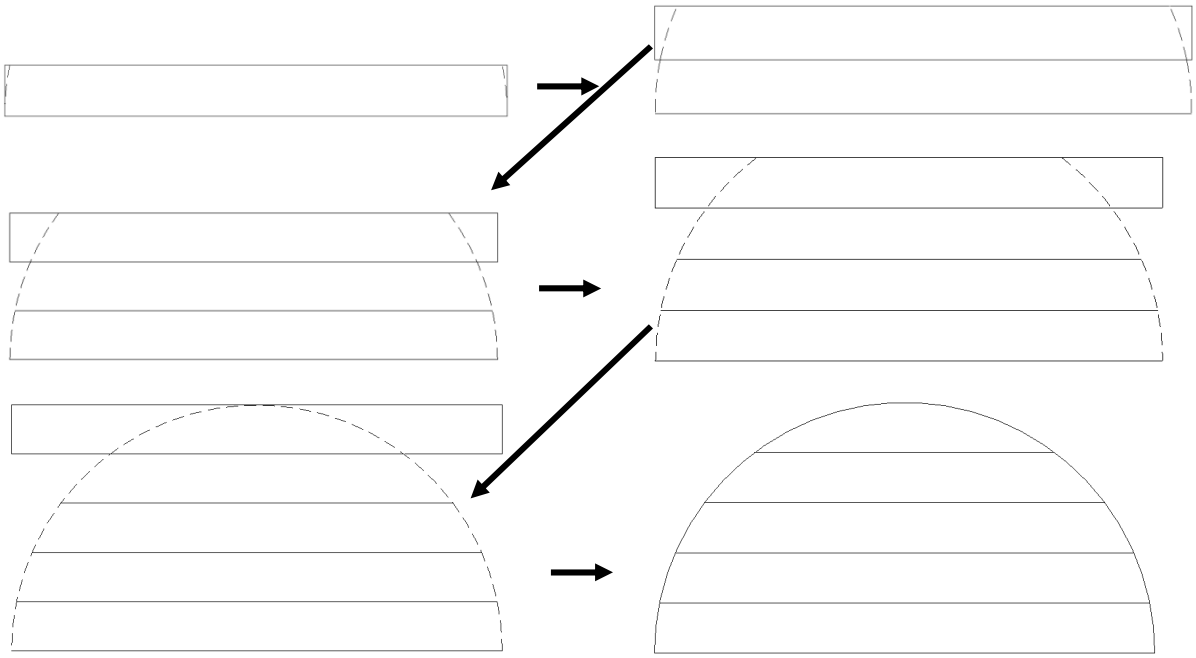

Figure 4. Hybrid process of machining geometry layer by layer

Recent literature has emerged to rapidly produce die tooling (discussed in further detail in Chapter 2). Both additive and hybrid approaches have been utilized. In general, additive approaches struggle to achieve sufficient interlaminate strength and often require complete surface machining or grinding. Some success has been shown with hybrid processes, though problems arise in interlaminate strength, layer registration, and assembly methods.

Laminated Die Motivation

Time and cost are the two primary drivers for rapid manufacturing. Hybrid rapid manufacturing of die tooling specifically addresses these two advantages. By decomposing die tooling into discrete layers and later joining them by mechanical means, advantages are realized both through the individual layers and the nature of assembly.

Decomposing dies into layers allows material-based advantages. First, stock material can be chosen that is large enough to manufacture a single layer, rather than being restricted to a large piece of stock that contains the largest dimension of the die. Second, a layer scheme

allows the designer to use different materials for each layer. Rather than machining the entire die tooling from a single hard material, the designer can specify non-critical layers as a less expensive and more machinable material.

Layer decomposition allows for simpler CNC machinery and process planning. Die tooling can have deep geometry, which can require long tools or multi-axis machines to manufacture as one piece. These factors increase cost and machining difficulties (i.e. chatter, machine stiffness, accuracy). In a layer-based strategy, each layer can be machined independently, allowing use of inexpensive three axis CNC mills and short, rigid tools.

The lead time to manufacture a layer-based die could be much shorter than that to manufacture a solid die. Outsourcing dies often require several weeks of lead time (Walczyk & Hardt, 1999). Shorter lead times are achieved through simple and robust process planning and the potential for parallel processing. The layered process has the ability to make different layers on different machines at the same exact time and assemble afterwards. The ability to send a 3D model of the die tooling to a CNC mill and receive final die tooling greatly shortens the time to manufacturing.

Finally, by mechanically joining layers, die tooling can be easily disassembled. This allows replacement of a single layer if it wears prematurely, or redesign and remanufacture of individual layers during iterations through process development. Bolt joining is a method that is versatile to different materials. Additionally, pins can be utilized for layer registration by aligning each layer.

Of the primary sheet metal forming operations, the presented work focuses on modeling stamping as a bending operation. Punching has nearly vertical forces which results in very little shear force and high compressive force acting on the die tooling. Drawing dies are rather simple and often symmetric. Bending operations are interesting in that it bends sheet metal at a point of contact that can create shear and compressive force off-balance. The off-balance in force components creates interesting process planning for interlaminate strength.

Thesis Objective

The objective of this research is to develop a process planning method for laminated die manufacture to automatically provide adequate interlaminate strength using a minimum number of fasteners. Based on inputs of die geometry, predetermined layer thickness, die material properties, predetermined hardware size, and sheet metal properties, the algorithms provided by this research will output specific bolt and dowel pin locations.

Constraints defined by Walczyk and Hardt state that laminated die tooling requirements include layer registration, layer bonding, interlaminate strength, disassembly, and automation (Walczyk & Hardt, 1998). To this end, one component of this research is the development of a model for determining interlaminate forces during sheet metal bending.

Thesis Scope

This research focuses entirely on dies for bending (as opposed to shearing or drawing). Laminated die architecture of horizontal layers, joined by dowel pins and bolts, is assumed in this work. By utilizing dowel pins and bolts, holes can be automatically drilled and reamed or tapped in the same CNC mill that creates each layer, satisfying the "automation" requirement for laminated die tooling. Further, the use of these two types of hardware allows easy disassembly of the die. By using at least two pins between each layer, the registration of each will be fully defined, and by using an appropriate number of bolts, the layers will be properly bonded to resist gravitational forces. Finally, by adding additional pins or bolts, the interlaminate strength during stamping can be adjusted. Thus, this configuration allows meeting each of the requirements for laminated tooling.

The presented work assumes that the die geometry, layer locations, hardware geometry, and sheet metal properties are predetermined. Since only bending dies are considered, the force analyses are justified in not considering the shearing or stretching of the sheet metal.

Thesis Organization

Chapter 2 provides a literature review of bulk and discrete methods for die tooling manufacturing. The review demonstrates the need for stiff, rapid die tooling. Chapter 3

presents the research problem. Chapter 4 presents original work in determining and overcoming the force and moment requirements for die tooling during sheet metal bending. Chapter 5 presents original work for bolt and layer placement in the previously described model. Chapter 6 is a case study of the original work. Chapter 7 is a discussion and future direction for the presented work.

Chapter 2. Literature Review

Previous endeavors into 'rapid' die tooling have generally followed two paths: (1) bulk tool manufacture and (2) discrete layer manufacture. The next two sections present the state of art in each area.

Bulk Tool Manufacture

Bulk tool manufacture results in a single contiguous piece of tooling. Permanently joining the layers via welding, brazing, or epoxy ensures adequate surface smoothness and interlaminate strength. Other methods consider sintering powder to develop the net-shape geometry.

One proposed method is to create a mold to cast die tooling. Casting die tooling is highly effective to replicate die geometry. Du *et al.* proposes an indirect method for rapidly producing die tooling from existing rapid prototyping methods (Du, Chua, Chua, Loh-Lee, & Lim, 2002). First, the female die half is made via stereolithography (SLA), selective laser sintering (SLS), or high speed CNC milling (Du, Chua, Chua, Loh-Lee, & Lim, 2002). Next, a negative of the geometry is cast into silicone rubber molds. Finally, vacuum casting was used to create a final tool in aluminum epoxy. Although authors note this method would not be adequate for mass production tooling due to the weak mechanical cast metal properties, the application of existing rapid manufacturing technologies were shown to create successful dies for low volume applications (Du, Chua, Chua, Loh-Lee, & Lim, 2002).

Rather than developing a mold, other researchers developed methods of directly depositing material to create solid die tooling. Hybrid-layered manufacturing (HLM) is a welding process that produces a near net-shaped layer and mills the desired geometry when complete (Akula & Karunakaran, 2006). HLM uniquely deposits direct metal onto each layer using existing technology. The HLM process for developing die tooling has several benefits compared to other existing rapid prototyping technologies capable of depositing metal – selective laser sintering (SLS) and 3-D printing (3DP). HLM is able to achieve better surface finish than SLS and 3DP because the final die is viewed as 'one slice.' The stair-stepped

surface is removed in the last process step whereas SLS and 3DP have a stair-stepped surface. Akula noted that desired die tooling material properties could not be attained by the welding process.

Discrete Layer Manufacture

Over the past 70 years, research has ventured into laminated tools. Laminated layer tools apply to many different applications. One of the first inventors to patent a layer-based mold to reproduce and reconfigure shoe soles appeared in 1942 (Hart, 1942). Hart recognized the labor time, inaccuracies, and cost associated with producing traditional shoe soles and developed a layer-based method. Hart developed locating plates for the layers to rest upon and a locating bar to ensure proper positioning. Disassembling and rotating the layers with proper location allowed Hart to produce a mirrored image of an asymmetric mold with accurate replications of shoe soles. Hart's shoe sole design had two main concepts that layer-based die tooling researchers have continued to follow: (1) layer reconfiguration, and (2) locating and positioning plates.

Clevenger *et al.* applied this concept of laminated plates to patent a method focusing only on hydraulic pressing sheets for female dies (Clevenger, Cohen, & Cohen, 1954). The hydraulic press creates a tight seal between the layers. Laminations are stacked with pins on opposite corners and hydraulically pressed into the previous layer for securing (Figure 5). Clevenger *et al.* suggests that the hydroforming process lends itself well to interchanging layers for multiple types of materials (steel, brass, aluminum, cardboard, paper, or plastics). Although Clevenger's concept suited well to multiple materials and disassembly, he did not consider mechanical requirements in his design.

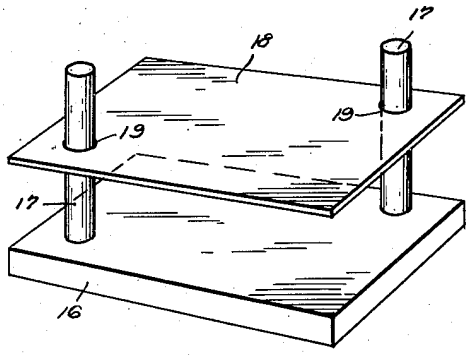

Figure 5. Locating pins for press fitting (Clevenger, Cohen, & Cohen, 1954)

DiMatteo addressed problems associated with three-dimensional shapes with unique cross-sectional geometry as well as accessibility issues associated with the depth of three-dimensional external and internal shapes (DiMatteo, 1976). DiMatteo developed a method for constructing three-dimensional bodies with decreased time requirements and cost. Layers were automatically cut using laser beam, mill, or saw X and Y coordinates on the surface. Once a layer was complete, a roller applied an adhesive to the cut layer. A new layer was then attached. In cases where metals are used, the layers were attached by a bolt that passes through all layers and secured with a nut on the opposite side. In the case of die tooling, layers were stacked and all the layers were bolted together noted by the four holes shown in Figure 6.

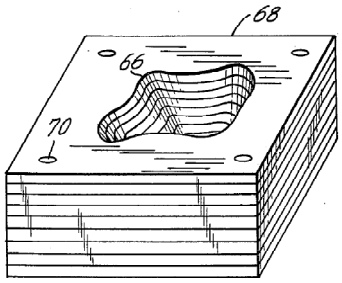

Figure 6. Female die for punch press (DiMatteo, 1976)

Walczyk and Hardt applied the concept of layer-based die fabrication and added a beveled curve to approximate the first-order interpolation of the surface to remove the stair-stepped look of traditional rapid prototyping dies (Walczyk & Hardt, 1998).

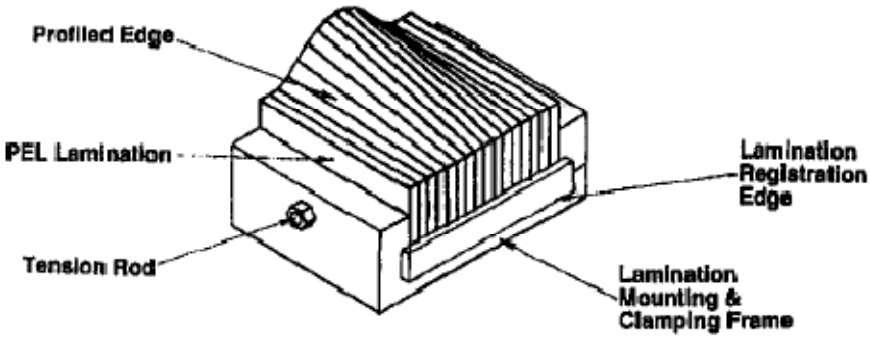

Figure 7. Profiled edge lamination (Walczyk & Hardt, 1998)

Vertical layer orientation encounters layer delamination from loading in the form of elastic deforming or buckling under loads (Walczyk & Hardt, 1998). Forces applied at the surface of the die, shown in Figure 8, include frictional force (μF_n) and the normal force (F_n). The buckling and bending forces from interlaminate layers can further be determined from the normal force and coefficient of friction (μ) (Walczyk & Hardt, 1998).

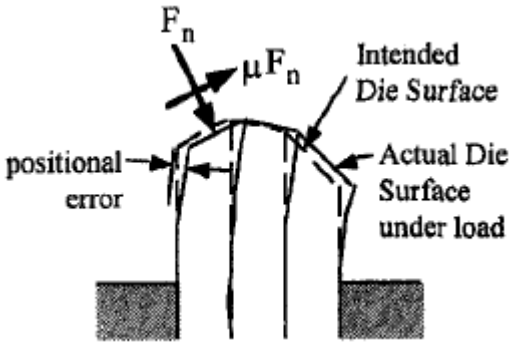

Figure 8. Vertical layer orientation delamination (Walczyk & Hardt, 1998)

Walczyk developed an analytical model to address the structural integrity of unbonded and adhesively bonded ANSI 6061-T6 aluminum layers in the vertical layer orientation (Walczyk & Im, 2005). The cantilever beam model evaluated deflection by varying the number of layers, layer thickness, and joining method when a force is applied across sheets of metal. Analytic and finite element models were validated with experimental data. The experimental validation mounted sheets of AISI 6061-T6 aluminum into a vise. The deflection error between the model and the experimental trials ranged between -25% and +12% error (Walczyk & Im, 2005). Walczyk and Im noted the high negative error was due to the overly stiff unbounded trials.

No method currently exists to build horizontal layers with increased layer strength. Although much force is applied in the z-axis, the surface geometry may lend to shearing forces which are cause for concern with layer slip or delamination. Without a proper analysis of the interlaminate strength with mechanical joining methods (pins and bolts), layer-based die tooling may not have the structural integrity of a permanent die.

Often, dies require several iterations before the correct die is developed. The ability to interchange layers for redesign is desirable and has been a motivating factor in previous research. Interlaminate strength by bolt would allow the interchange of layers. The use of bolts as a joining method for rapid fabrication for dies is not a new concept. However, previous research has not focused on the interlaminate strength of a bolt securing method. Proper strength should eliminate slippage and delamination from forces in sheet metal operations. One of the primary areas of this research is on interlaminate shear stresses in die tooling.

Advantages and Problems with Laminate Dies

Walczyk and Hardt have published the most extensive papers in the area of laminated tooling (Walczyk & Hardt, 1998), (Walczyk & Hardt, 1999), (Im & Walcyzk, 2002), (Shook & Walczyk, 2004), (Walczyk & Im, 2005), (Yoo & Walczyk, 2005), (Walczyk & Yoo, 2009). Walczyk and Hardt (Walczyk & Hardt, 1998) describe four main advantages of the vertical layer orientation versus the horizontal layer orientation. The first advantage is that the

profiled-edge lamination can be automated easily to slide on the locating plates since only the top surface is cut, leaving datum surfaces on the bottom and sides of each layer. The horizontal layers are more difficult to automate the layer material handling. The second advantage that is the sheets are located on the surfaces of the lamination mounting and clamping frame to ensure location and position, as shown in Figure 7. The horizontal method is difficult to locate (particularly in the case of islands). The third advantage is ease of securing by clamping force. The horizontal method is difficult to secure each layer. Lastly, the vertical layers lend to easy reconstruction. Removal of layers requires simple unclamping of the vise.

Chapter 3. Research Problem

Notation

Geometric properties:

- P_i Point on slice parameter
- D_{BZ} Bolt zone diameter
- D_{PZ} Pin zone diameter
- S_i Span length

Mechanical properties:

- F_m Layer mass force
- M_{L_i} Moment for layer and side i

Hardware:

- D_B Bolt head diameter
- D_P Pin diameter
- N_B Number of bolts
- N_P Number of pins

Interface Shear:

- F_f Frictional force
- μ Coefficient of friction

Interface Moment:

- M_{L_i} Moment about layer L
- L_h Layer height
- L_w Layer width

Pin:

- F_p Pin force
- γ_y Pin material shear yield strength
- N_P Number of pins
- r_p Radius of pins

Bolt:

- F_B Bolt preload tensile force
- d_{B_i} Moment arm distance to bolt$_i$
- σ_U Ultimate tensile stress (bolt)
- $F_{PRELOAD}$ Preload force
- A_s Tensile stress area

Layer Weight:

- m Layer mass
- F_m Layer mass force
- ρ_w Density
- V Volume of layer

Laminated Die Architecture

The objective of this research is to develop a process planning method for laminated die manufacture to automatically provide adequate interlaminate strength using a minimum number of fasteners. From Walczyk's work (Walczyk & Hardt, 1999), laminated die tooling requires four essential elements: (1) automation, (2) layer registration, (3) securing for tool rigidity, and (4) disassembly. Laminated die tooling with horizontal layers can be rapidly manufactured for sheet metal bending based on predetermined inputs of die geometry, predetermined layer thickness, die material properties, predetermined fastener size, and sheet metal properties. Outputs from this system include the number and location of the fasteners within each interlaminate surface.

The hardware presented in this study includes dowel pins and bolts. Two dowel pins meet Walczyk's second element of layer location. If only one dowel pin were used, interlaminate rotation will occur, Figure 9a. Bolts meet the fourth element of die disassembly. Additional dowel pins and bolts can achieve tool rigidity under predetermined force conditions. Bolts serve as a joining tool that allows for easy disassembly of the die tooling. Mechanically, bolts also serve as a resistance to layer rotation along the frontal plane, Figure 9d.

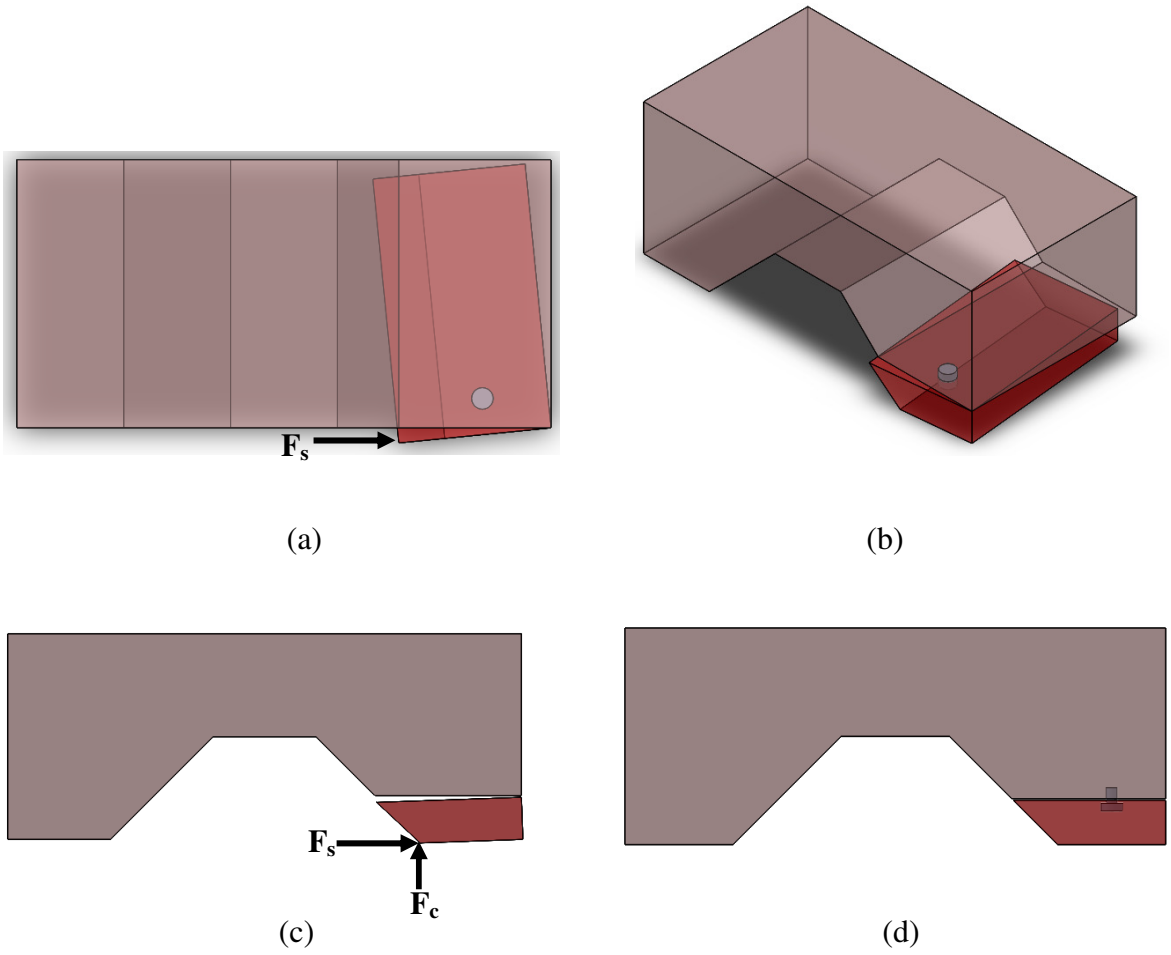

Figure 9. (a) Top view of die with translation rotation from only one pin, (b) isometric view of translation rotation, (c) front view of die with frontal rotation without joining, and (d) front view of frontal rotation with bolt

However, without proper design for mechanical requirements, the die tool may not be rigid. Shear (F_s) and compressive (F_c) forces are shown as black arrows acting on one layer of the

laminated die tooling during sheet metal bending, Figure 10a. The beam balancing arrows to create a static layer from the shear and compressive forces are displayed in red. Mechanically, dowel pins serve as resistance to layer sliding shown in Figure 10b. However, dowel pins are not enough to resist the moment acting on the layer as a result of the shear and compressive forces magnitude. A moment about the layer may still occur without proper number and positioning of bolts, Figure 10c. Based on bolt properties, the bolt will act as a counteracting force on the layer's moment, Figure 10d.

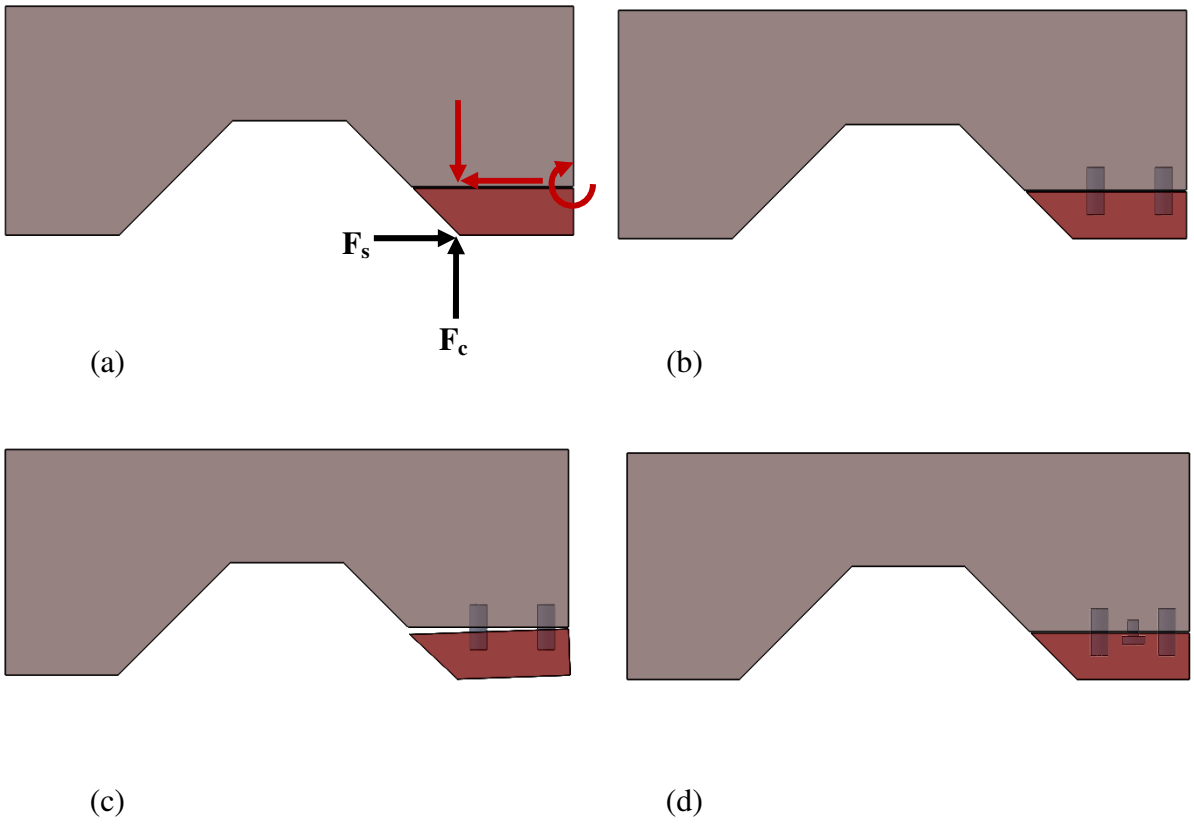

Figure 10. (a) Forces from sheet metal to the die (black) and counteracting forces from die to sheet metal (red), (b) dowel pins resist shear force, (c) dowel pins do not resist moment, and (d) bolt to resist the moment

Formal Problem Statement

The objective of the proposed system is to minimize the quantity of bolts and dowel pins per layer subject to the following design constraints:

- Spacing hardware
- Locate layers
- Bond layers
- Resist interlaminate shear
- Resist interlaminate moment

To develop a formal problem statement, each constraint must be examined and quantified. The following sections address each constraint individually.

Hardware Spacing

Safe distance from the layer edge allows for proper thread engagement for bolts and material thickness for dowel pins. Safe distance between hardware is ensuring that bolts and dowel pins are not too close to one another. Applying hardware to two layers allows for the system to have a standard bolt and dowel pin size. When placing the hardware to layers, the above layer cannot overlap the hardware. If so, hardware interference is created.

Bolts and dowel pins cannot be too close to one another. The following work refers to the bolt as the "bolt zone" and the dowel pin as the 'pin zone.' The bolt has a diameter, D_B, which is largest at the bolt head. The additional zone (D_{BZ}) is the physical diameter around the bolt head end is the minimum distance any feature can be from the bolt. The dowel pin operates in the same fashion. The dowel pin has a nominal diameter, D_P, with an additional zone (D_{PZ}) surrounding the dowel pin diameter. The zones (D_{BZ} and D_{PZ}) will be predetermined by the operator.

(a) (b)

Figure 11. (a) Bolt head (solid line) with additional bolt zone (dotted line) and (b) dowel pin (solid line) with additional dowel pin zone (dotted line)

Locating Layer

Dowel pins will both locate layers with respect to one another and prevent interlaminate sliding from shear force in this technology. Based on these expressions, the number of interlaminate pins can be derived. The minimum number of pins can be determined for the die tooling in equation 1.

$$N_p \geq Safety\ Factor \cdot \frac{F_s - \mu \cdot F_c}{\gamma_y \cdot A} = Safety\ Factor \cdot \frac{F_s - \mu \cdot F_c}{\gamma_y \cdot (\pi {r_p}^2)} \quad (1)$$

Where:

$F_s = Shear\ Force$

$F_c = Compressive\ Force$

$\mu = Coefficient\ of\ static\ friciton\ between\ layers$

$\gamma_y = Pin\ material\ yield\ strength$

$N_p = Number\ of\ pins$

$A = Cross\ sectional\ area\ of\ pin$

$r_p = Radius\ of\ dowel\ pin$

From equation 1, the theoretical minimum number of dowel pins required to resist shear force can be obtained. However, additional dowel pins may be required to accommodate for the die tooling layer geometry and to resist translation rotation.

Layer Bonding

The interlaminate joint strength is critical. The bolt is the primary securing mechanism in the proposed system. Without a bolt, the die tooling layer is not properly secured. In this case, the bolt tensile force is the mass of the current and the previous layers (F_m), shown in equation 2.

$$F_m = \rho_w \cdot \sum_{j=i}^{n} V_j \tag{2}$$

Where:

$$\rho_w = Material\ density$$

$$V_i = Volume\ of\ layer\ i$$

The force on the bolt (F_B) must be less than the tensile force experienced on the bolt. If F_B is greater than the tensile force, the bolt will break (Bickford, 2008).

$$F_B < \frac{(\sigma_U - F_{PRELOAD})(A_S)}{Safety\ Factor} \tag{3}$$

Where:

$$\sigma_U = Ultimate\ Tensile\ Stress\ of\ bolt$$

$$F_{PRELOAD} = Preload\ force\ required\ when\ bolting\ (equation\ 4)$$

$A_s = Tensile\ stress\ area\ (equation\ 5)$

$Safety = Safety\ factor$

Equation 4 requires knowledge of the preload force when joining the layers. Required preload force can be obtained from equation 4 (Bickford, 2008):

$$F_{PRELOAD} = K_B \cdot P \cdot \frac{\theta_R}{360} \tag{4}$$

Where:

$K_B = Bolt\ stiffness$

$P = Pitch\ of\ threads$

$\theta_R = Angle\ of\ nut\ rotation\ (degree)\ with\ respect\ to\ the\ bolt$

The bolt force also requires knowledge of the tensile stress area. The tensile stress area of a standard 60° thread bolt is determined from equation 5 (Bickford, 2008):

$$A_s = \frac{\pi}{4}\left[D - \left(\frac{0.9745}{n}\right)\right]^2 \tag{5}$$

Where:

$D = nominal\ diameter$

$n = number\ of\ threads\ per\ inch$

The bolt stiffness is given in equation 6 below (Bickford, 2008).

$$K_B = \frac{EA_s}{L_C} \tag{6}$$

Interlaminate Shear Forces

The layers experience interlaminate shear force from sheet metal bending. The shear force results in the layers sliding past one another. Interlaminate frictional force influences is one component that influences shear force. The layer free body diagram in Figure 12 displays the frictional force vector occurring on the interlaminate surface. The frictional force vector is directed opposite of the shear force from bending the sheet metal. In turn, the frictional force decreases interlaminate stress and is vital to include in force modeling.

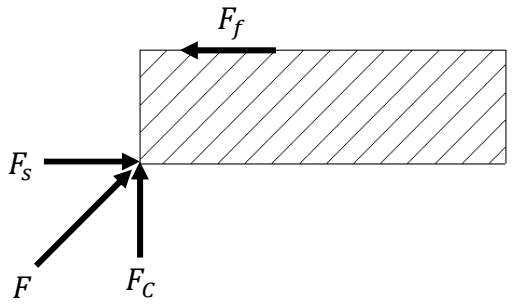

Figure 12. Free body diagram of interlaminate forces

The coefficient of friction between die layers (μ) creates a force opposite F_s, proportional to F_c, that helps resist the tendency of F_s to shift layers relative to each other. The frictional force is the resistance from side movement due to the material relationship from the coefficient of static friction (μ).

$$F_f < \mu \cdot F_c \tag{7}$$

Pins are designated to resist the interlaminate shear force. As the coefficient of friction between each layer, μ, approaches zero, the force on the pins increases.

$$Pin\ Shear\ Force = F_P = F_s - F_f = F_s - \mu \cdot F_c \tag{8}$$

The number of pins can be simplified from equation 1.

$$N_p \geq Safety\ Factor \cdot \frac{F_P}{\gamma_y \cdot (\pi {r_p}^2)} \quad (9)$$

Figure 13a demonstrates a case where the shear force exceeds the frictional force. Pins are used to overcome plate sliding from shear force in Figure 13b.

(a) (b)

Figure 13. (a) Shear force applied to bottom layer causes sliding and (b) pins (n) resist shear force

Effect of Sheet Metal and Die Tooling Friction

Friction exists between the sheet metal and the die tooling. Figure 14 displays the free body diagram of the forces acting on the die tooling from the sheet metal. As shown, the frictional force ($F_f = \mu F_c$) acts opposite shear force (F_s) and with compressive force (F_c). From $F_p > F_s - \mu F_c$, reducing F_s and increasing F_c has the effect of reducing the pin shear force (F_P).

In the presented work, frictional force between the sheet metal and the die tooling is considered to be negligible for model simplification. Neglecting frictional force also provides a worst-case scenario; this will result in a conservative estimate of total pin force. In reality, the shear force experienced by the pins may be smaller.

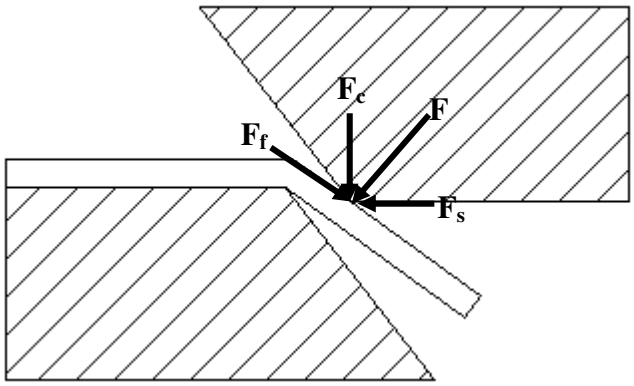

Figure 14. Free body diagram between sheet metal and die tooling

Layer Moment

Layer moment is the last mechanical requirement analyzed in the presented system. Layer moment is crucial for process planning to prevent delamination of layers.

Layer Moment Calculation

In the presented work, bolts are utilized to resist the moment acting on each layer during sheet metal bending. While dowel pins and bolts both resist forces in multiple directions (with varying degrees of success), their effects are separated to simplify the analysis and provide a worst-case bound.

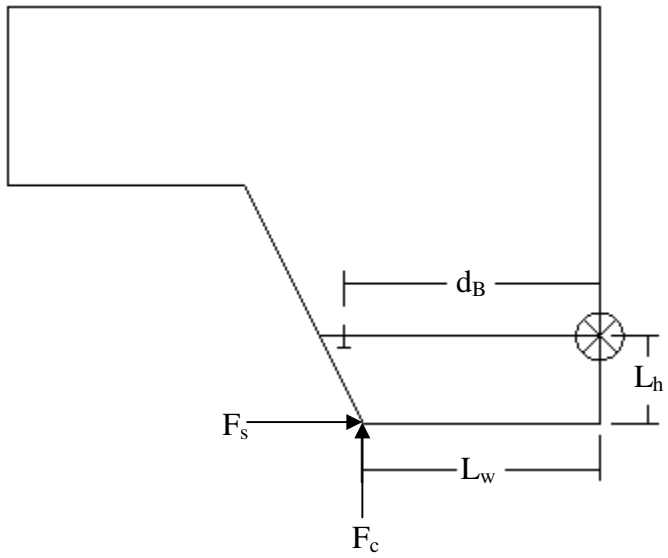

Figure 15. Layer moment with bolt resistance

Figure 15 displays the moment acting on layer i from shear and compressive forces. The layer moment occurs when $F_s L_{h_i} > F_c L_w$. Bolts resist the moment by tensile force (F_B) and the bolt distance from the moment.

The resultant layer moment, i, acting on a given layer, j, for all bolts, k, is given in equation 10.

$$M_{L_i} = F_{s_j} \cdot L_h - F_{c_j} \cdot L_w \leq F_{B_k} \cdot \sum d_{B_k} \tag{10}$$

Where:

$F_s = Shear\ force$

$F_c = Compressive\ force$

$F_B = Bolt\ tensile\ force$

$L_h = Layer\ height$

$L_w = Layer\ width$

$d_{B_k} = Moment\ arm\ distance\ to\ bolt_i$

Bolt Force

Based on the expression $\sum d_B \cdot F_B \geq F_s \cdot L_{h_i} - F_c \cdot L_w$, the number of bolts can be determined. Unlike the number of pins, satisfying the moment condition is dependent on the physical location of the bolt within the slice geometry.

Revisiting the Formal Problem Definition

Having defined each constraint, the mathematical problem definition is provided below.

Objective Function: Minimize the N_B and N_P in L_i

Constraints:

(1) Safe distance from slice edge:
   - From slice edge to bolt: $P_i - D_B \geq D_{BZ}$
   - From slice edge to pin: $P_i - D_P \geq D_{PZ}$

(2) Safe distance between hardware:
   - Between bolts: $D_{B_i} - D_{B_j} \geq D_{BZ}$
   - Between pins: $D_{P_i} - D_{P_j} \geq D_{PZ}$
   - Between bolts and pins: $\left|D_{B_i} - D_{P_i}\right| \geq MAX(D_{BZ}, D_{PZ})$

(3) Resist interlaminate shear: $N_p \geq \frac{MAX\left(\left|F_{P_{Di}}\right|,\left|F_{P_{Dj}}\right|,\ldots,\left|F_{P_{DN}}\right|\right)}{\gamma_{y\cdot(\pi r_p{}^2)}}$

(4) Locate layer: $N_p \geq 2$

(5) Resist interlaminate moment: $\sum d_B \cdot F_B \geq F_s \cdot L_{h_i} - F_c \cdot L_w$

(6) Satisfy layer weight criteria: $\sum d_B \cdot F_B \geq F_m$

(7) Space bolt location along largest span: $MAX(S_i, \ldots, S_N)$

Research Direction

The number of dowel pins and bolts are easily derived. The only unknown solving for the number of dowel pins and bolts is determining the shear (F_s) and compressive (F_c) force components. Previous researchers have not considered the shear and compressive forces at any height during sheet metal bending. Knowing proper force components during sheet metal bending, die tooling fastener placement is determined to withstand layer sliding and layer moment. Chapter 4 derives the shear and compressive forces for two arbitrary geometries. After determining these forces, a heuristic method for solving the best location for the dowel pins and bolts is determined. Two algorithms are proposed in Chapter 5 for the placement of bolts and dowel pins.

Chapter 4. Modeling Die Tooling Requirements in Sheet Metal Bending

The objective of this research is to develop a process planning method for laminated die manufacture to automatically provide adequate interlaminate strength using a minimum number of fasteners. Chapter 3 discusses the primary problem in determining the minimum number of fasteners which is determining the correct force modeling of the die tooling surface. Chapter 3 presents the basic form of the shear force and layer moment equations. This chapter derives the basic equations for different geometries. Chapter 5 uses the shear force and layer moment expressions determined in this chapter as inputs for a process planning algorithm for die manufacture. This chapter presents an original contribution of a mechanical analysis for die tooling considering only the effect of mechanical loads on the tooling during sheet metal bending.

Force models exist for modeling sheet metal bending. Boothroyd (Boothroyd, Knight, & Dewhurst, 2002) modeled the required force to bend sheet metal as the average compressive force from strain energy. Boothroyd's model does not account for shear force, which is important for the proposed model. Walcyzk and Im (2005) modeled layer deflection as a result of a known force input. The presented model here determines both the mechanical shear and the moment from an unknown force input based on die tooling geometry.

A review of past work does not reveal a mechanical model that determines the required forces to bend sheet metal based on die tooling geometry. Horizontal layers are prone to failure mode if the maximum mechanical requirements are not adequately modeled. Compression from bending sheet metal will be absorbed by the horizontal layers just as in a traditional die. However, the horizontal component of sheet metal bending will act on the die tooling in a direction that would cause the layers to shear apart. In other cases, these forces can cause layers to rotate with respect to each other. Determining the maximum shear and moment loads experienced by the die tooling for different die tooling geometries is important to prevent tool failure.

Overview of Modeling Methodology

Designing for mechanical requirements extend the functionality of rapid die tooling. The shear force results in sliding of layers while the moment results in rotations of layers. Both the shear force and moment must be controlled to prevent delamination of the die layers during use. The two primary mechanical requirements of concern in the presented work for horizontal laminated die tooling are the shear force and moment as previous shown in Figure 10.

Input geometry determines the required force to bend sheet metal in the presented work. Two geometries are presented in this work: linear and parabolic. A linear surface is a simple case where the surface of the die tooling may have varying slopes. Parabolic surfaces are modeled to represent sheet metal bending about a curved surface. Parabolic surfaces are the most tractable of conical shapes. Parabolic surfaces fit to a variety of curved surfaces to predict force components. Although linear and parabolic surfaces are the only geometries discussed in the presented work, the present model can be adapted to model other surfaces.

The remainder of this chapter covers the necessary steps for modeling shear force and layer moment. The next is an overview of the variables presented in this chapter followed by a discussion of the general force model to bend sheet metal. Next, the force model verification is discussed. Lastly, the mechanical requirements are concluded.

Notation

Sheet metal properties:

- W Width of sheet metal
- σ_y Yield strength (sheet metal)
- t Sheet metal thickness
- E Young's modulus (sheet metal)

Bending Moment:

- M Moment of sheet metal about the die tooling

- I Moment of inertia
- ρ_C Radius of curvature

Contact Forces:

- F Resultant force
- F_s General shear force component
- F_c General compressive force component
- F_f Frictional Force
- $F_{s(L)}$ Linear shear force component
- $F_{s(P)}$ Parabolic shear force component

Die Geometry:

- C Height of the geometry
- A Width of die geometry
- D_F Distance Factor

Sheet Metal Bending Moment

The sheet metal can be modeled as a simple beam bending problem where the moment to bend the sheet metal is the bending force times the moment arm distance. The sheet metal moment arm can be determined by pre-existing calculations. However, for curvature, the moment arm may contain parts of plastic and elastic deformation.

The required force to bend the sheet metal can be determined from beam bending equations. Figure 16 displays the moment to plastically bend sheet metal about the neutral axis.

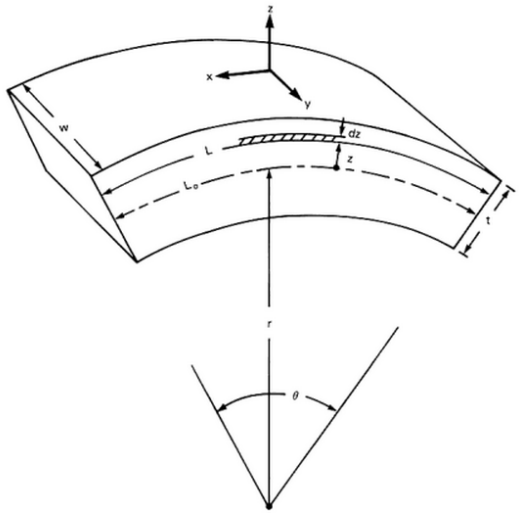

Figure 16. Moment to plastically bend sheet metal (Hosford & Caddell, 2007)

Assuming purely plastic deformation of the sheet metal around a sharp corner or tight radius for linear geometry, the moment can be calculated as shown in equation 11 (Hosford & Caddell, 2007).

$$M = \int (stress)(area)(moment\ arm) = \int_{-t/2}^{t/2} \sigma_y W\, z\, dz \tag{11}$$

Where:

$$\sigma_y = Yield\ stress\ of\ sheet\ metal$$

$$W = Width\ of\ sheet\ metal$$

$$z = Interval\ +\frac{t}{2}\ to\ -\frac{t}{2}$$

Simplification of the sheet metal moment arm equation 11, can be resolved in equation 12, (Hosford & Caddell, 2007).

$$M = 2\int_0^{t/2} (\sigma_y)(W\, dz)(z) = \frac{\sigma_y W t^2}{4} \tag{12}$$

The moment from equation 12 occurs for linear geometry where the point of rotation is near zero. Sheet metal bending about a curved surface follows a different moment arm equation if elastically deformed. For an elastic bending situation, the moment is evaluated in equation 13 (Shigley, 1956).

$$M = \frac{EI}{\rho} \tag{13}$$

Where:

$$E = Young's\ Modulus$$

$$I = Moment\ of\ inertia$$

$$\rho = Radius\ of\ curvature$$

Since the sheet metal is assumed to be a rectangle, the moment of inertia for a rectangular section can be substituted into equation 14 and further be expanded.

$$M = E \cdot \frac{Wt^3}{12} \cdot \frac{1}{\rho} \tag{14}$$

The radius of curvature can be expanded to include the surface geometry to give the final moment shown in equation 15 (Stewart, 2009).

$$M = E \cdot \frac{Wt^3}{12} \cdot \frac{\frac{d^2y}{dx^2}}{\left(1+\left(\frac{dy}{dx}\right)^2\right)^{3/2}} \tag{15}$$

General Force Model

As previously discussed, the sheet metal bending moment is one of two input parameters to determine sheet metal bending force. The second input parameter is the moment arm distance. The moment arm distance is dependent on the die tooling geometry.

The resultant force is the total force required to bend the sheet metal. Shear force is one component of the resultant force. Knowing the resultant force, the shear force can be derived. The die corner will have some finite radius and the force will be normal to the sheet metal. Thus, the resultant force is always normal to the sheet metal as shown in Figure 17.

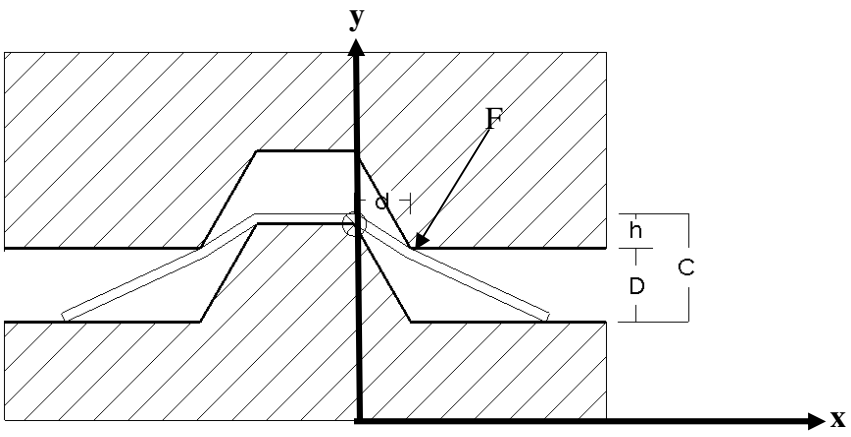

Figure 17. Reacting Force Normal to Sheet Metal

Die tooling variable definitions include (illustrated in Figure 17):

- d – Distance from between die halves points of contact
- C – Height of the geometry
- h – Distance moved by the top die
- D – Vertical distance between die halves

The second input parameter to determine the resultant force is the distance. The resultant force to bend sheet metal for the above geometry is given in equation 16 below.

$$F = \frac{M}{\sqrt{d^2+h^2}} \tag{16}$$

Reaction Force

The resultant force can be decomposed into compressive (F_c) and shear (F_s) force components. Compressive and shear forces are modeled from the point of contact with the sheet metal as shown in Figure 18.

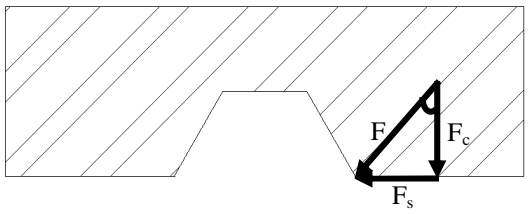

Figure 18. Resultant force and x and y force components acting on the sheet metal through the point of contact

Algebraically, the resultant force can be resolved into shear and compressive force components:

$$F_s = F\sin\theta = \frac{M}{\sqrt{d^2+h^2}} * \frac{h}{\sqrt{d^2+h^2}} \tag{17}$$

$$F_c = F\cos\theta = \frac{M}{\sqrt{d^2+h^2}} * \frac{d}{\sqrt{d^2+h^2}} \tag{18}$$

The force acting on the pin is determined in equation 19.

$$F_p = F \cdot \sin\theta - F \cdot \mu \cdot \cos\theta = F\left(\frac{h-d\mu}{\sqrt{d^2+h^2}}\right) = M\ \frac{h-d\mu}{d^2+h^2} \tag{19}$$

Piece-wise Linear Die Model

The previous discussion developed general models for determining F_s and F_c (equations 17 and 18) as a function of die shut height D and parameters d and h shown in Figure 19. This section develops particular solutions for d and h based on linear edge die geometry.

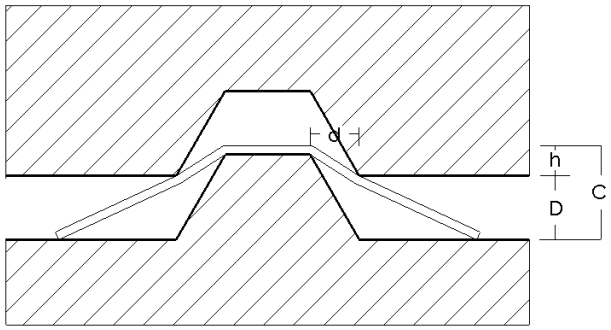

Figure 19. Variables *h* and *D* change with time during bending

A geometric relationship between shear force (F_s) and stamping height D for a linear surface can be determined by the geometric die height C. As the die stamps sheet metal, the resultant force remains constant, but the shear and compressive forces alter as the die height is reduced. For piecewise linear geometry, the die surface can be described in equation 20, where C represents the maximum height of the die and A_L is the slope of the linear surface.

$$y = -A_L x + C \rightarrow 0 < x < \left(\frac{C}{A_L}\right) \tag{20}$$

From equation 20, variables d and h are defined for linear geometry as given in equations 21 and 22 below. The variable d is the point of contact distance on the sheet metal from the top to the bottom die. The variable h is the distance the top die has moved downward during clamping.

$$d = \frac{C}{A_L} \tag{21}$$

$$h = C - D \tag{22}$$

Substituting linear equations for d and h into the original shear and compressive force expression on the dowel pin (equations 17 and 18), equations 23 and 24 are determined.

$$F_{S(L)} = M \cdot \frac{h}{d^2+h^2} = M \cdot \frac{(C-D)}{\left(\frac{C}{A_L}\right)^2+(C-D)^2} \tag{23}$$

$$F_{c(L)} = M \cdot \frac{d}{d^2+h^2} = M \cdot \frac{\left(\frac{C}{A_L}\right)}{\left(\frac{C}{A_L}\right)^2+(C-D)^2} \tag{24}$$

The shear force acting on the dowel pins for a linear surface includes frictional force as shown in equation 25.

$$F_{P(L)} = M \cdot \frac{h-d\mu}{d^2+h^2} = M \cdot \frac{(C-D)-\left(\frac{C}{A_L}\right)\mu}{\left(\frac{C}{A_L}\right)^2+(C-D)^2} \tag{25}$$

Parabolic Die Model

Modeling parabolic surfaces follows the same steps as the linear model. First, the resultant force is determined from the surface geometry. The parabolic shear force is a component of the shear force.

Parabolic Resultant Force

Modeling curvature in sheet metal bending is more complex than linear surface. Similar to linear surface, curvature can be modeled using equation 16 for the resultant force, $F = \frac{M}{\sqrt{d^2+h^2}}$. This analysis becomes more difficult because the point of contact on both die halves is continuously changing as shown in Figure 20; both h and d will now be functions of D.

Whereas previously h was determined by a single contact point on the bottom die, it now must be found so that the contact point satisfies a tangent boundary condition as the sheet is formed over the die.

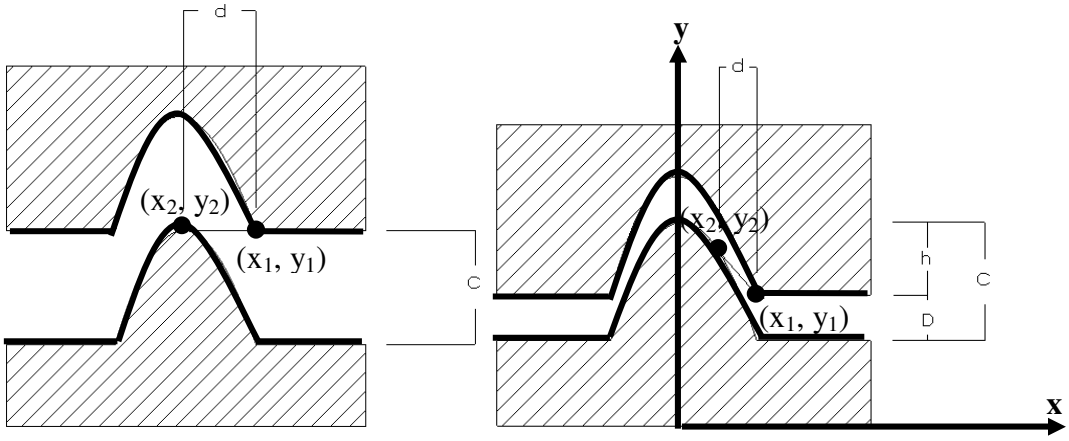

Figure 20. Continuously changing tangent slope and point of contacts for a parabola

The basic equation for the surface of the downward parabola is $y = -Ax^2 + C$ where A is the focus (parabola width) and C is the parabola height. The minimum moment required to bend the sheet metal for a parabola is assumed to trade between plastic and elastic deformation, provided in equations 12 and 15. If the radius of curvature is large, the sheet metal may not completely plastically deform. In this case, sheet metal springback occurs. The moment arm is continually changing for parabolic die geometry. The force required to plastically deform the sheet metal is different based on the equation for a parabola. The ratio of h and d can be equated to the slope of the lower die at the contact point, thus allowing the contact point to be determined algebraically:

$$slope = \frac{dy}{dx} = \frac{-h}{d} = \frac{y_1 - y_2}{x_1 - x_2} = -2Ax_2 \tag{26}$$

From equation 26, x_1 and y_1 are determined at the maximum x and y values along the tangent. The equations for x_1 and y_1 are given in equations 27 and 28 respectively.

$$y_1(x_1) = 0 \Rightarrow x_1 = \sqrt{\frac{C}{A}} \tag{27}$$

$$y_1 = D \tag{28}$$

Substituting the values for x_1 and y_1, while replacing y_2 with the standard equation for a parabola, $-Ax_2^2 + C$, into the slope equation, equation 29 can be derived.

$$slope = \frac{D-\left(-Ax_2{}^2+C\right)}{\sqrt{\frac{C}{A}}-x_2} = -2Ax_2 \tag{29}$$

Solving for x_2 in equation 28 gives the final expressions for h and d which are given in equation 30 and 31.

$$h = 2\sqrt{CD} - 2D \tag{30}$$

$$d = \sqrt{\frac{D}{A}} \tag{31}$$

Now, the parabolic surface is in terms of the linear surface (h and d). The values from h and d can be substituted into the expression for general resultant force (equation 16) to obtain the resultant force for a parabolic surface:

$$F = \frac{M}{\sqrt{d^2+h^2}} = \frac{M}{\sqrt{\left(\sqrt{\frac{D}{A}}\right)^2+\left(2\sqrt{CD}-2D\right)^2}} \tag{32}$$

Valid Bound on Force

The sheet metal moment about a parabolic surface is unlike that of a linear surface. As the moment approaches zero, $\lim_{M\to 0} Undefined$, the moment is undefined. The sheet metal experiences both plastic and elastic moments about the parabolic surface. The moment arm (d) for the parabola approaches zero. The model must account for sheet metal thickness as the die tooling is clamping for a curved surface.

The top die will stop at some D value above zero. Offsets to accommodate for the sheet metal thickness should be considered for a further, more accurate model. To determine the height at which the top die theoretically stops, an offset normal to the parabolic surface equal to t is projected outward, shown in Figure 21.

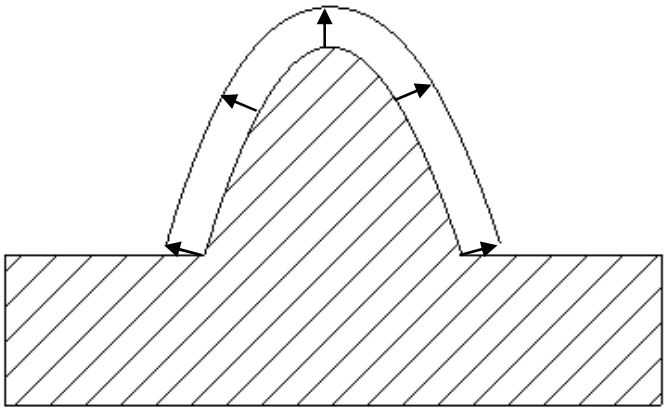

Figure 21. Sheet Metal Thickness Offset

The slope of the line created from the end points of the two parabolas can be derived from the first derivative of the equation of the parabola.

$$m = -2Ax \tag{33}$$

The previous equation expands by substituting the x value:

$$m = -2A\sqrt{\frac{C}{A}} \tag{34}$$

The final slope for the line is given in equation 35.

$$m = -2\sqrt{CA} \tag{35}$$

Once the slope and offset of the parabola have been determined, the angle between the base of the die tooling and the slope can be derived, noted as θ. Figure 22 is a visual representation of the sheet metal and the h and d values.

$$\theta = \tan^{-1} m \tag{36}$$

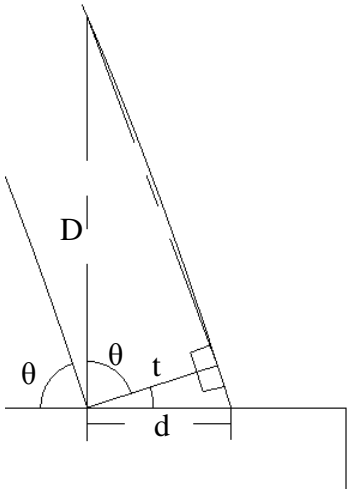

Figure 22. Determine minimum d and D values for a parabola

The shutting height, D, that accounts for the sheet metal thickness is given in equation 37.

$$D \geq \frac{t}{cos\theta} \tag{37}$$

Determine Parabolic Shear Force

The original shear and compressive forces determined in equations 17 and 18 are evaluated for the parabolic surface resultant force, equations 38 and 39.

$$F_{s(P)} = Fsin\theta = \frac{M}{\sqrt{\left(\sqrt{\frac{D}{A}}\right)^2 + \left(2\sqrt{CD} - 2D\right)^2}} \cdot \frac{\left(2\sqrt{CD} - 2D\right)}{\sqrt{\left(\sqrt{\frac{D}{A}}\right)^2 + \left(2\sqrt{CD} - 2D\right)^2}} \tag{38}$$

$$F_{c(P)} = Fcos\theta = \frac{M}{\sqrt{\left(\sqrt{\frac{D}{A}}\right)^2 + \left(2\sqrt{CD} - 2D\right)^2}} \cdot \frac{\sqrt{\frac{D}{A}}}{\sqrt{\left(\sqrt{\frac{D}{A}}\right)^2 + \left(2\sqrt{CD} - 2D\right)^2}} \tag{39}$$

Following the same free body diagram in Figure 12, the total pin force for a parabola including frictional force expressed in equation 40.

$$F_{P(P)} = F \cdot sin\theta - F \cdot \mu \cdot cos\theta = M\left(\frac{\left(2\sqrt{CD} - 2D\right) - \left(\sqrt{\frac{D}{A}}\right)\mu}{\left(2\sqrt{CD} - 2D\right)^2 + \left(\sqrt{\frac{D}{A}}\right)^2}\right) \tag{40}$$

Determine Shear Component Maximum

Ideally, an expression can be derived to determine the maximum shear force on the die tooling given the input geometry. The shear force is continually changing with the changing resultant force. If a mathematical expression for maximum shear force exists for either the linear or parabolic models, the modeling is greatly simplified.

Shigley (Shigley, 1956) presented a way of determining the maximum deflection for a beam bending model. Shigley performed the first derivative test of the distance criteria function. The maximum deflection occurs at the peak of the function when the slope is zero. This is known as the first derivative test for engineering mechanics.

Similar to Shigley's first derivative test for maximum deflection, maximum pin force acting on the die tooling layers can be determined by use of the first derivative test. The height D at which the pin force is highest can be determined through the first derivative test.

Linear Geometry Maximum Pin Force

The following expressions test for the local maximum pin force for a linear surface as the shut height, D, changes. D is defined as the clamping distance between die halves. The first derivative test equates the pin force of the linear surface as a function of the shutting height and sets the first derivative equal to zero as shown in equation 41.

$$\frac{dF_{P(L)}}{dD} = 0 \tag{41}$$

The first derivative of the total pin force, given in equation 41, is evaluated in equation 42.

$$\frac{\mathrm{dF_{P(L)}}}{\mathrm{dD}} = M \frac{\mathrm{d}}{\mathrm{dD}} \frac{(C-D)-\left(\frac{C}{A_L}\right)\mu}{\left(\frac{C}{A_L}\right)^2+(C-D)^2} \tag{42}$$

Equation 42 can be solved and reduced to a simple equation for maximum pin force applied to the die tooling for linear geometry:

$$F_{P(L),max} = M\left(\frac{A_L}{2C}\right)\left(\frac{1}{\sqrt{\mu^2+1}+\mu}\right) \tag{43}$$

The shutting height D of the maximum pin force is shown in equation 44.

$$D = C - \left(\frac{C}{A}\right)\left(\mu + \sqrt{\mu^2+1}\right) \tag{44}$$

The detailed calculations for deriving the linear surface first derivative are in Appendix I. First Derivative Test: Linear Surface.

Parabolic Geometry Maximum Shear Force

No common factors cancel when expanding the parabolic shear force expression to create a $(C - D)$ relationship. The derivative can be calculated in a straightforward manner, but it is impractical to solve for D such that the derivative equals zero, much less substitute the resulting value for D back into the original equation. The maximum pin force for a parabola is highly dependent on the input parameters (A and C). Thus a graphical approach is taken to finding the maximum pin force by varying input parameters A and C.

Since the parabolic surface could not obtain a maximum pin force, the pin force is graphed to determine the maximum pin force.

$$Parabolic\ Edge\ Distance\ Factor: \frac{\left(2\sqrt{CD}-2D\right)-\left(\sqrt{\frac{D}{A}}\right)\mu}{\left(2\sqrt{CD}-2D\right)^2+\left(\sqrt{\frac{D}{A}}\right)^2} \tag{45}$$

Graph Parabolic Surface

The force behavior of the parabolic edge differs from the linear edge. When graphing, the minimum of the plastic and elastic shear force values were used as D approached zero. This accounts for springback that may occur during the bending process. The following series of figures (Figure 23 and Figure 24) display the change of the shear force as two die halves clamp onto the sheet metal. The following example maintains a constant t and A, 0.0625 inches and 0.0625 inches^{-1} respectively. The graph shown in Figure 23 begins with a negative pin shear force (F_P), meaning that the die is initially stable without pins. As the die reaches D = 7.5 inches, the pin shear force begins to increase.

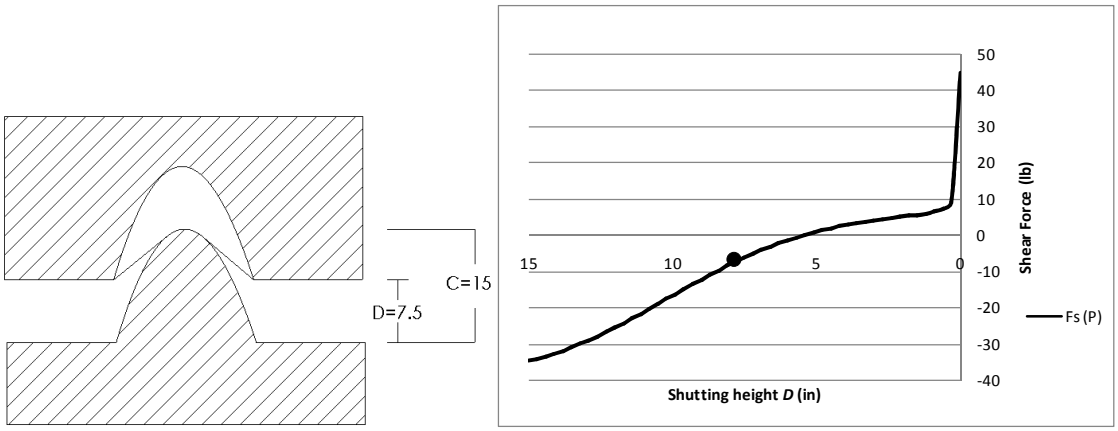

Figure 23. Bending Sheet Metal about Parabola (D = 7.5 in.)

As the die tooling is fully clamped, the pin shear force experienced by the die spikes significantly, shown in Figure 24 and becomes non-existent at $D = 0\ inches$. Based on the graph, no quantity of pins will be able to resist the pin force from the spike. The spike reaches an infinite shear force.

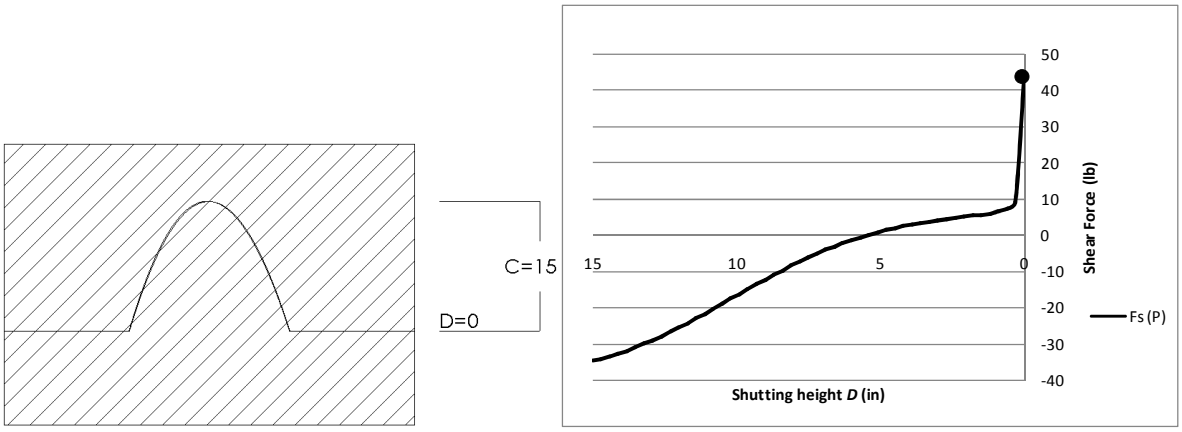

Figure 24. Bending Sheet Metal about Parabola (D = 0 in.)

Now, adjusting for the invalid moment, the D for this particular case derived from equation 36, is $D = 0.14\ inches$.

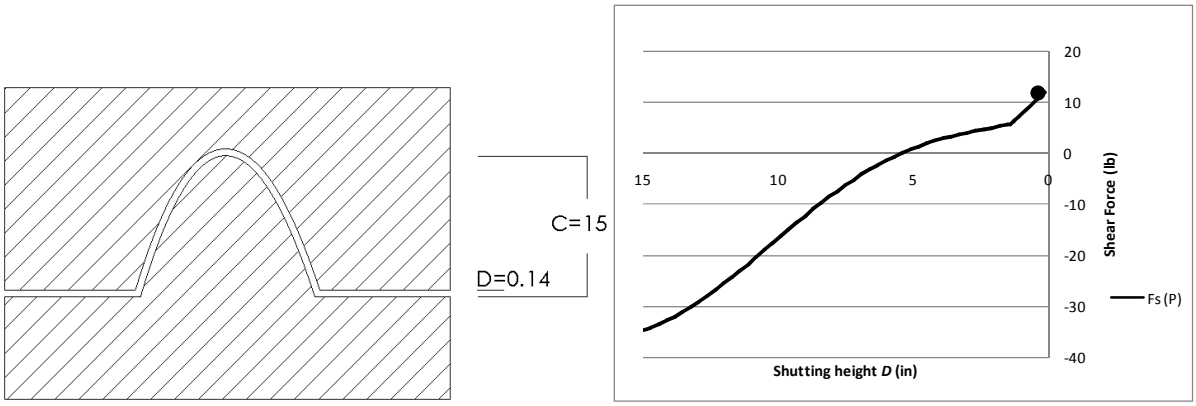

Figure 25. Bending Sheet Metal about Parabola (D = 0.14 in.)

The presented approach estimates shear force for a parabolic surface. More complex modeling to include sheet metal thickness offsets could be developed for a more accurate representation.

Force Model Verification

The previously discussed model presents a method for predicting shear forces and layer moments based on die tooling geometry. The number of bolts and pins has been determined throughout this chapter. The distribution and location of bolts and pins to satisfy the mechanical requirements will further be discussed in Chapter 5.

Similar to the proposed model, different models have been developed to analyze required forces for sheet metal bending. Previous work in sheet metal bending did not combine shear force, compressive force, and resultant force based on the die geometry at any point in time. However, previous authors can guide the presented work for general solutions.

Boothroyd modeled sheet metal bending as the required work done by unit volume. This model determines the average compressive forces. The average compressive force can determine the desired press for a given sheet metal bending operation. The pitfall of this model is it does not provide force components over bending time for process planning.

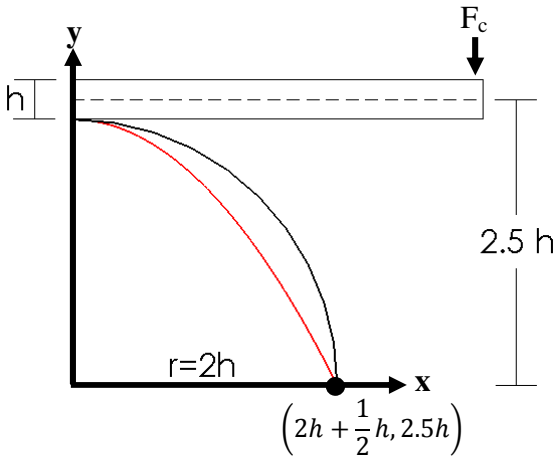

Figure 26. Fitting parabola curve (red) to arc (black) (Boothroyd, Knight, & Dewhurst, 2002)

According to Boothroyd, the average compressive force determined by work done by unit volume is given in equation 46 (Boothroyd, Knight, & Dewhurst, 2002).

$$F_c = 0.08 \cdot U \cdot h \cdot L_b \tag{46}$$

Where:

$$U = Ultimate\ Tensile\ Strength$$

$$h = Sheet\ Metal\ Thickness$$

$$L_b = Width\ of\ the\ Sheet\ Metal$$

For a stainless steel die with U = 95,000 lb/in^2 (Groover, 2002), h = 0.0625 inches, and L_b = 8 inches. The average compressive force is calculated in equation 47.

$$F_c = 0.08 \cdot 95{,}000 \frac{lb}{in^2} \cdot 0.0625\ in \cdot 8\ in = 3{,}800\ lb \tag{47}$$

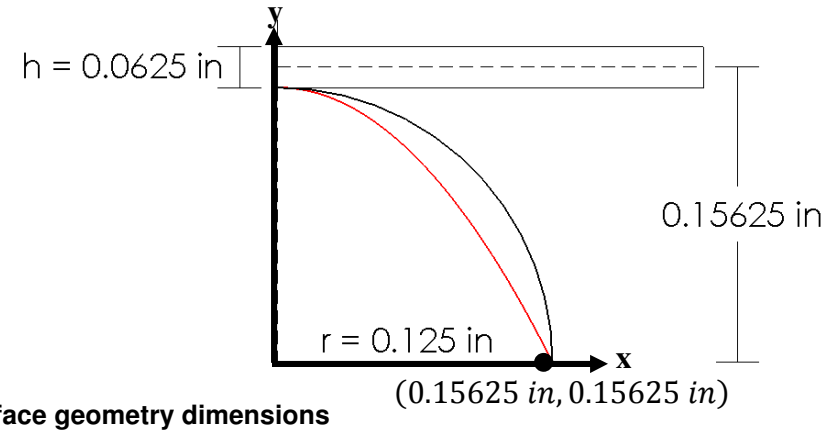

Figure 27. Surface geometry dimensions

Using the dimensions in Figure 27 for the compressive force calculation in the presented work, the compressive force can be determined at any point in time. A is determined in equation 48.

$$\sqrt{\frac{C}{A}} = C \rightarrow A = \frac{1}{C} \tag{48}$$

All variables are known for the parabolic compression force, given in equation 49.

$$F_{c(P)} = F\cos\theta = M \cdot \frac{\sqrt{\frac{D}{A}}}{\left(\sqrt{\frac{D}{A}}\right)^2 + \left(2\sqrt{CD} - 2D\right)^2} \tag{49}$$

The dark blue line is the change in compressive force over the change in D. The light blue line is the average compressive force. The red line is the average compressive force from the strain energy equation (Boothroyd, Knight, & Dewhurst, 2002). For the given variables, the average compressive force by the parabola is 5,024 lb.

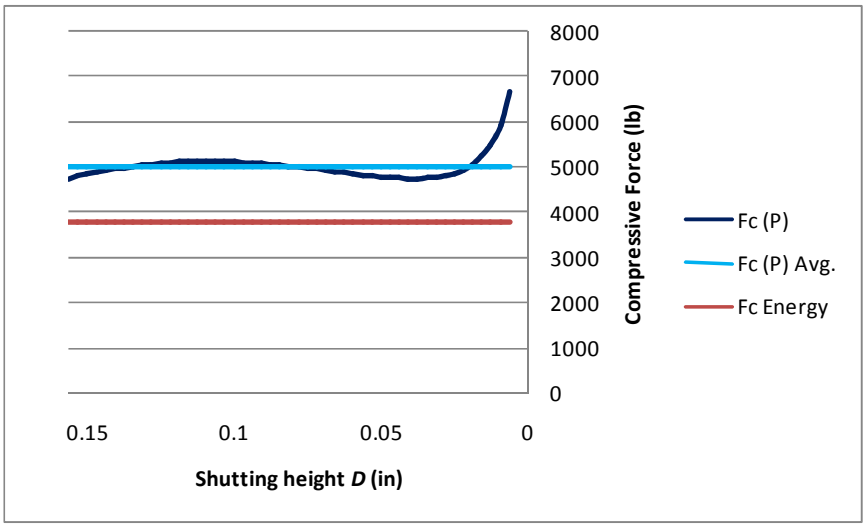

Figure 28. Compressive force from parabolic and strain energy equations

Mechanical Requirements Conclusion

The primary objective of this research is to develop a process planning method for die manufacture, with improved interlaminate stress compared to existing methods. Chapter 4 accomplished the first half of this objective by determining the interlaminate shear and moment vectors for laminated tooling.

Interlaminate shear forces were evaluated from a simple beam bending model. Original contribution from this the presented work is the interlaminate force analysis modeled from the sheet metal bending moment and the die tooling surface geometry. Two types of geometry were analyzed: linear and parabolic. The first derivative test determined the maximum shear force applied to a linear surface, but was unable to provide a solution for the parabolic surface. The maximum shear force for a parabolic surface is determined by graphing the shear force against the shut distance, *D*. Following the force modeling, layer moment modeling was determined for both linear and parabolic surfaces.

Based on the mechanical requirements formed from the shear force and layer moment equations, expressions for the number of bolts and pins per layer were derived. The number of bolts and pins from Chapter 4 serves as an input for the bolt and pin placement algorithm presented in Chapter 5.

Chapter 5. Bolt and Pin Placement Algorithm

As proposed in Chapter 3, bolts and pins can be used to resist the moment and shear force (respectively) between the die tooling layers. Chapter 4 presented an analysis to determine the magnitude of these forces and moments for two different geometry types: linear and parabolic. This chapter presents an algorithm for placing fasteners to meet mechanical requirements. The presented work is a heuristic of the interlaminate requirements for die tooling geometry.

The presented algorithm is designed to import a stereolithography (STL) file of the die tooling. A STL file is a polygon surface approximation of the 3D model called tessellation. When creating a slice along the z axis through the STL file, specific parametric points along the perimeter of the slice can be evaluated. Tessellation creates a discrete piecewise surface that can be simpler to analyze than a parametric surface.

This chapter analyzes the 3D model as a STL file. The slice parameter is an approximation of the true surface. The bolt and dowel pin locations are a result of the polygon surface approximation.

Notation

Geometric properties:

- P_i Point on slice parameter
- D_{BZ} Bolt zone diameter
- D_{PZ} Pin zone diameter
- S_i Span length

Mechanical properties:

- F_m Mass force
- M_{L_i} Moment for layer and side i

Hardware:

- D_B Bolt head diameter
- D_P Pin diameter
- N_B Number of bolts
- N_B Number of pins

Problem Formulation

Assuming dowel pins only affect shear and locating, and bolts only affect the moment and weight, the original objective function proposed in Chapter 3 can be divided into two independent objective functions: one for placing bolts and another for pins. These two independent optimization functions loop until all mechanical requirements are satisfied. Thus, the original problem proposed in Chapter 3 is decomposed into the following separate problems:

Objective function: Minimize the N_B in L_i

A1. Safe distance from slice edge:
   a. From slice edge to bolt: $P_i - D_B \geq D_{BZ}$

A2. Safe distance between hardware:
   a. Between Bolts: $D_{B_i} - D_{B_j} \geq D_{BZ}$

A3. Resist interlaminate moment: $M_{L_i} = F_s \cdot L_{h_i} - F_c \cdot L_w \leq \sum d_B \cdot F_B$

A4. Satisfy weight support: $\sum d_B \cdot F_B \geq F_m$

A5. Space bolt location along largest span: $MAX(S_i, \dots, S_N)$

Objective function: Minimize the N_P in L_i

B1. Safe distance from slice edge:
   a. From slice edge to dowel pin: $P_i - D_P \geq D_{PZ}$

B2. Safe distance between hardware:
   a. Between Dowel Pins: $D_{P_i} - D_{P_j} \geq D_{PZ}$

b. Between Bolts and Dowel Pins: $\left|D_{B_i} - D_{P_i}\right| \geq MAX(D_{BZ}, D_{PZ})$

B3. Resist interlaminate shear: $N_p \geq \frac{MAX\left(\left|F_{s_{Di}}\right|,\left|F_{s_{Dj}}\right|,\ldots,\left|F_{s_{DN}}\right|\right)}{\gamma_{y\cdot(\pi r_p{}^2)}}$ (equation 15 and 60)

B4. Satisfy feature locating: $N_p \geq 2$

The proposed algorithms use a heuristic method, where one optimization problem is solved completely before the next optimization problem. Further, a single layer is completely solved before progressing to the next. The success of minimizing either objective function is improved with a larger geometric feasible space. Thus, assuming no undercuts, the smallest geometric feasible space occurs on the layers that contact the sheet metal first. The moment constraint depends on the geometric location of the bolts, whereas the shear force is not dependent on the geometric location of the pins. Furthermore, placing dowel pins first reduces the geometric feasible space for bolts. Pins only require that the geometric feasible space exists. Therefore, the bolting algorithm is solved first

Bolt Location Algorithm

A flowchart of the presented bolt location algorithm is provided in Figure 29. The remainder of this section will step through each part of the algorithm in greater detail.

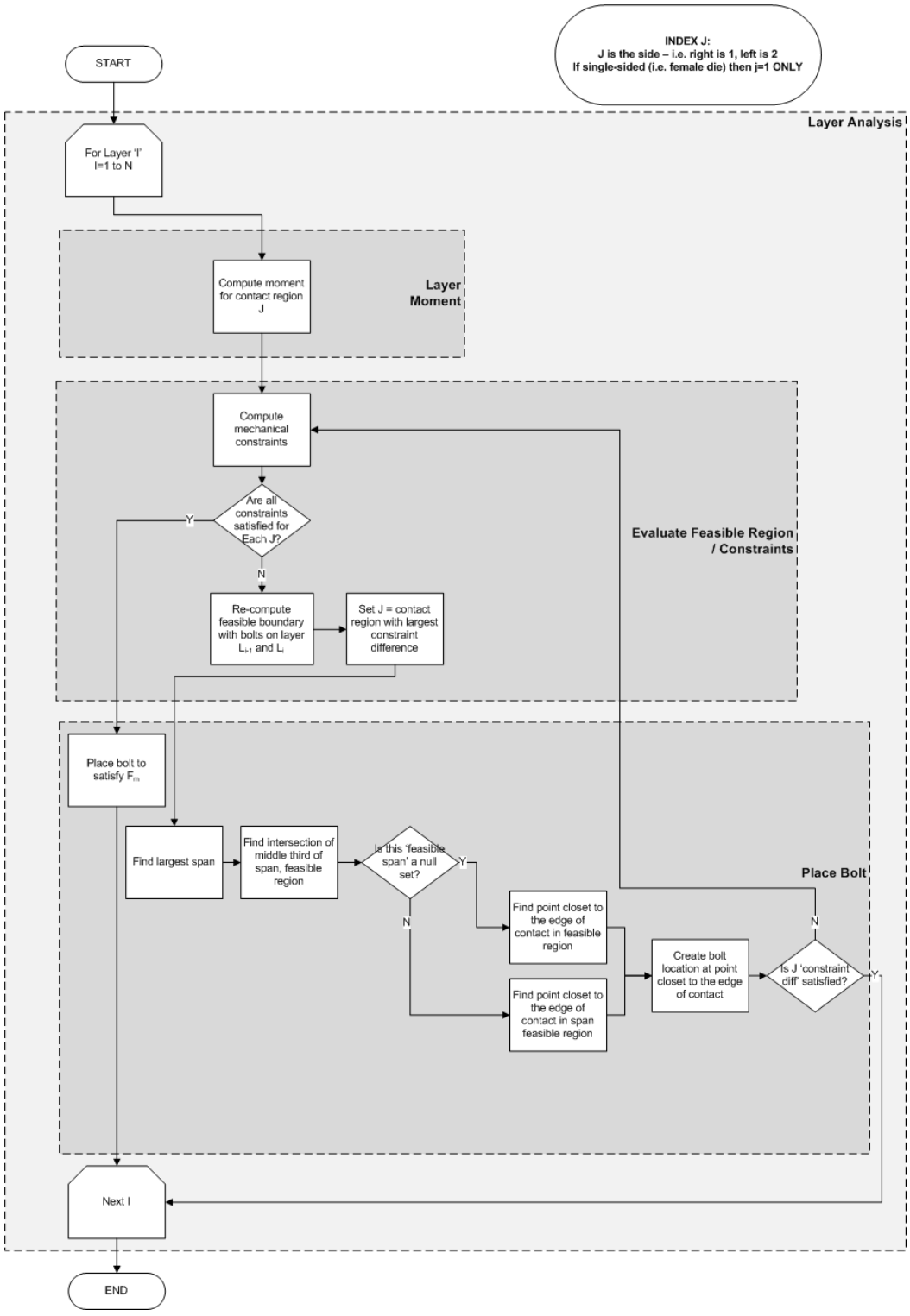

Figure 29. Bolt Location Algorithm

Layer Analysis

The presented algorithm loops for layers 'i' from 1 to N. The smallest geometric feasible space occurs at layers first to contact the sheet metal. The algorithm analyzes from the contact layer and continues until no additional layers exist to allow the geometric feasible region to grow from layer to layer. If no layers exist, the layer analysis can stop looping and the program can terminate.

Within the layer analysis, there are three primary subsections: layer moment, evaluate feasible region/constraints, and place bolt. These subsections loop until all moments within a layer are satisfied.

Layer Moment

As previously stated, the presented algorithm applies to any arbitrary, non-undercut edge for the 'contact region.' The contact region is the edge of the die that comes in contact with the sheet metal. The layer moment for the current layer is based on the summation of the previous layer thicknesses and the width for the layer at the point of contact. The calculation for the moment arm for each layer is discussed in Chapter 3, equation 9. Moment constraint, A3, is calculated for each layer.

Evaluate Feasible Region/Constraints

The mechanical constraint for the bolt algorithm includes moment and weight support. If the weight support greater than the moment, then the weight support is evaluated for the layer; otherwise the moment is evaluated for the layer mechanical constraints. When there are two contact regions, two moments will occur and counteract on one another. Therefore, solving for the contact region with the highest moment potentially satisfies the other contact region.

If the moment does exist, 'feasible region' is implied on the slice. A feasible region is a slice boundary offset. Boonsuk developed offset boundaries for locating sacrificial supports within the feasible region of the slice in his research (Boonsuk & Frank, 2009). Similar to Boonsuk's research, an offset of the intersection between the two layers will be developed.

The offset distance from the slice boundary is equal to D_{BZ}. The safety factor is a set distance that a feature can be from the bolt head.

The algorithm will create a Boolean operation to determine the current $L_i$offset: $L_{i-1} \cap L_i$ for $i = 1 \ldots n$. If n is zero, the union is ignored. If the previous layer has bolts ($L_{i-1} \ldots L_N$), the boundary will be developed around the previous layer's (L_{i-1}) bolt locations based on the union of the offset boundaries.

For a given z height, an offset of the slice boundary is projected inward. The z height and offset boundary are both predetermined by the user. The offset feasible region for L_i is defined as the intersection of hardware in L_{i-1} and the slice boundary of L_i. This prevents hardware from overlapping in layer interfaces. Hardware secures only two layers together to create less variability in the choices of hardware and securing locations.

Place Bolt

Find the largest span

The slice is first divided into a span (S_i). The span length is the vertical distance along the y axis shown in Figure 30.

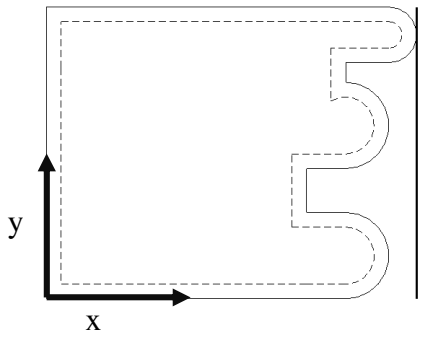

Figure 30. Bolt black line along the contact edge is the span

The largest span is chosen for evaluation: $MAX(S_i, \ldots, S_N)$. The divide occurs through the center of a bolt, Figure 31.

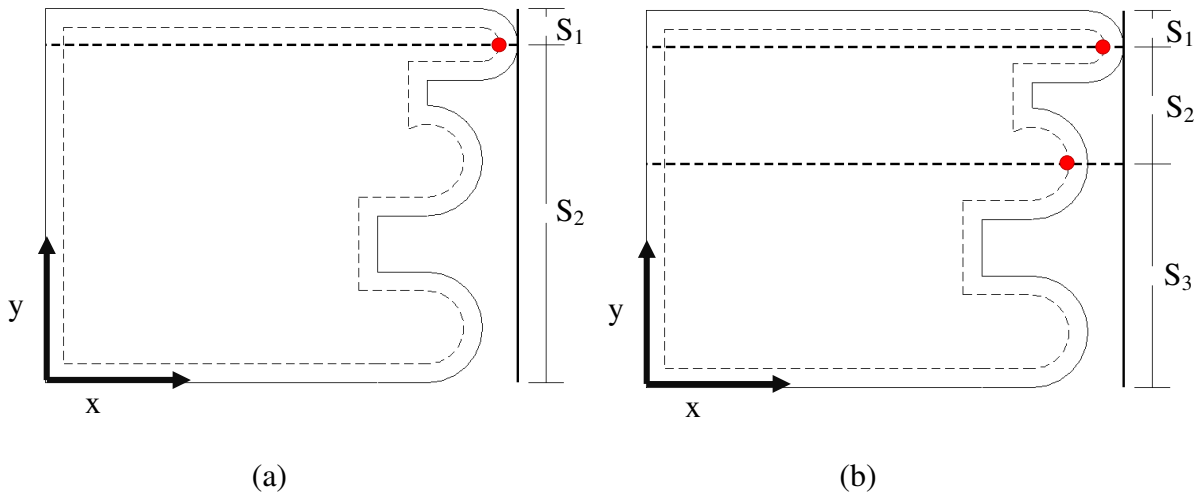

Figure 31. Spans shown for (a) 1 bolt and (b) 2 bolts. Note that if there are *n* bolts, then there are *n*+1 spans.

Find intersection of middle third of span, feasible region

The geometric constraint at minimum requires a safe distance offset between hardware (constraint A2). Even though the algorithm assumes a rigid body for bolting, the system would rather have bolts spread out than clumped right next to one another. Although satisfying the layer moment constraint requires placing bolts on the feasible region closest to the contact edge, the bolts should not be clumped next to one another. The middle 1/3 of the largest span is chosen to search for points on the feasible region closest to the contact edge as a method of spacing the bolts along the feasible region. The middle third of the largest span is an arbitrary zone size. If middle 1/3 is too restrictive, the zone could be changed to the middle 1/2. Since one bolt is placed at a time, the one third distance rule allows the minimum distance between hardware to be one third of the largest span's distance. The middle 1/3 satisfies that hardware will not be placed within one third of the largest distance. The middle 1/3 prevents bolts from being located too close to one another. The first bolt is placed by sectioning the layer into thirds as shown in Figure 32.

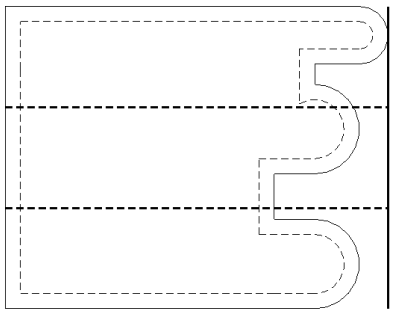

Figure 32. Middle third of slice – bold dotted lines is the middle third zone, bold solid line is the span

Is this 'feasible span' a null set?

In some cases, the middle zone may not exist as shown in Figure 33b. If this occurs, a search line will determine the highest point of the edge shown in Figure 33c. The search line is a straight edge, parallel to the contact edge of the die tooling.

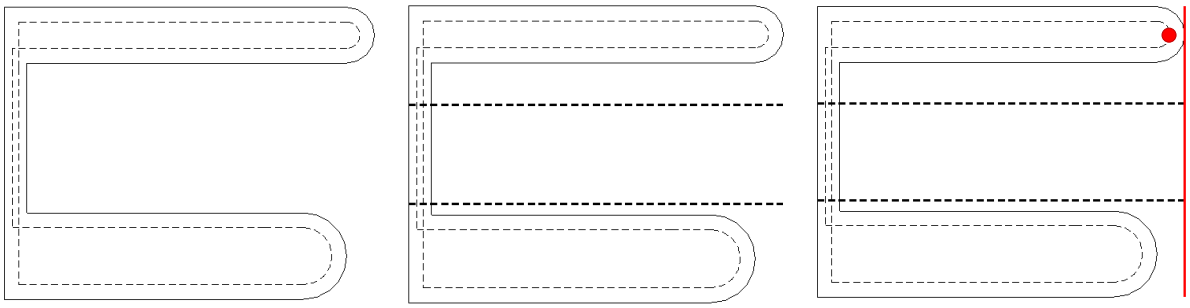

(a) (b) (c)

Figure 33. (a) Slice with offsets, (b) middle third zone, and (c) search line to find highest point outside middle zone

Find highest point in span feasible region

If the middle third is not a null set, the highest point of the middle third is determined. To offset a moment in the standard moment constraint, A3, the moment arm distance (d_{B_k}) should be as high as possible. In the slice coordinate system, the y-axis is parallel to the

contact edge, Figure 34. The distance along the x-axis in the middle third zone must be as large as possible to offset the predetermined layer moment.

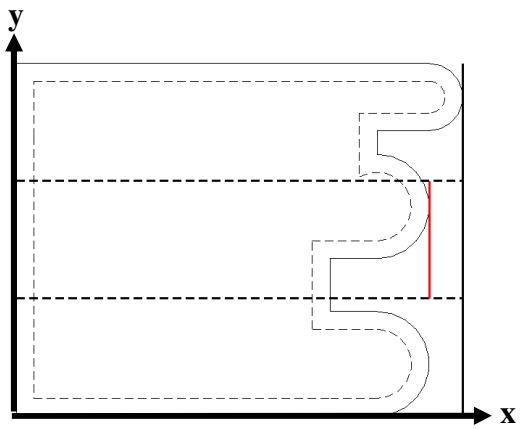

Figure 34. Slice x and y coordinate system

Create bolt location at point closest to contact edge

The bolt is placed on the offset boundary at the shortest distance from the point closest to the contact edge in the middle third, shown in Figure 35b. Once the bolt is placed, the moment arm will be calculated to determine if it is satisfied.

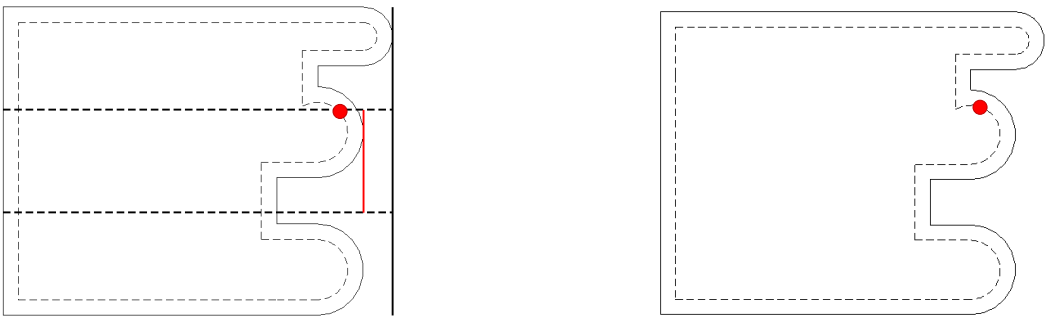

(a) (b)

Figure 35. (a) Search line searches for point closest to the contact edge and (b) bolt is placed at highest point

The point closest to the contact edge in any geometry can occur in three different ways: one point, multiple points, and straight line. If the highest point chosen is a single point, determining the bolt location is relatively easy. If multiple points are detected at the same height within the zone, only one point can be chosen, Figure 36a. For simplicity, the point nearest the center of the zone is chosen. If a straight line is detected in the zone, the bolt will be placed on the center of the offset boundary, Figure 36b.

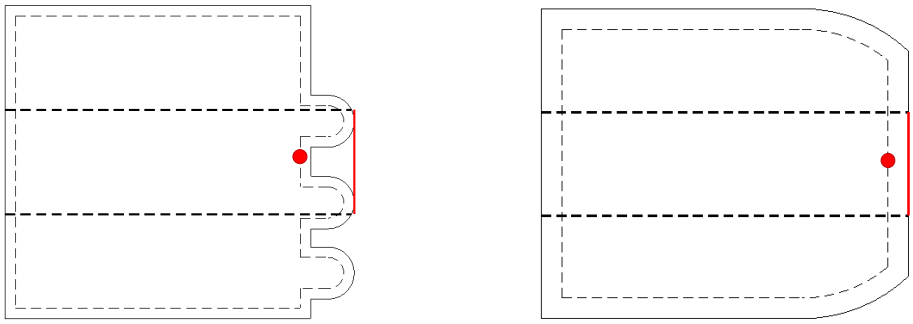

(a) (b)

Figure 36. (a) Multiple points detected and (b) a straight line detected

After the bolt is created at the slice high point, the algorithm loops back to the 'Evaluate Feasible Region/Constraints' section. If the bolt does not satisfy the mechanical constraints, an additional bolt must be placed on the slice. In this case, a span slit is introduced to evenly space the bolts. Figure 37a displays the first bolt placed by the previous condition. The dark dotted line is the bolt's location with respect to the slice width, creating two spans. The larger of the two spans is chosen for the split – in this case, the top span. Figure 37b shows the middle third of the span being chosen for the search line (shown in red). The middle third is always chosen to ensure that a series of bolts are not placed directly next to each other. The highest point is selected for the second bolt location.

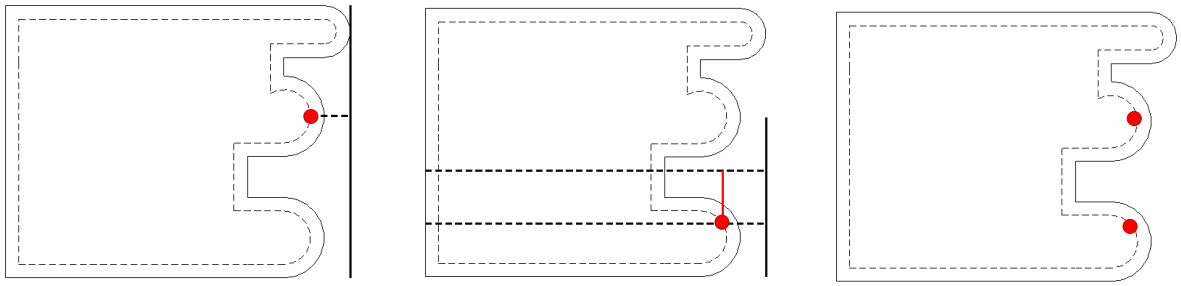

(a) (b) (c)

Figure 37. (a) Defining spans, (b) middle third of largest span and use search line for highest point, (c) place second bolt at this location

After the second bolt is placed on the slice, the slice is reevaluated for the moment condition. If the second bolt does not satisfy the moment condition, a third bolt must be placed on the slice. Any number of bolts after the first bolt follows the same span splitting conditions. Figure 38a displays the span split for the previous bolts. A search line detects the highest the highest point within the middle third of the largest span, Figure 38b. The highest point is chosen for the location of the third bolt. Span splitting continues until the layer moment is satisfied.

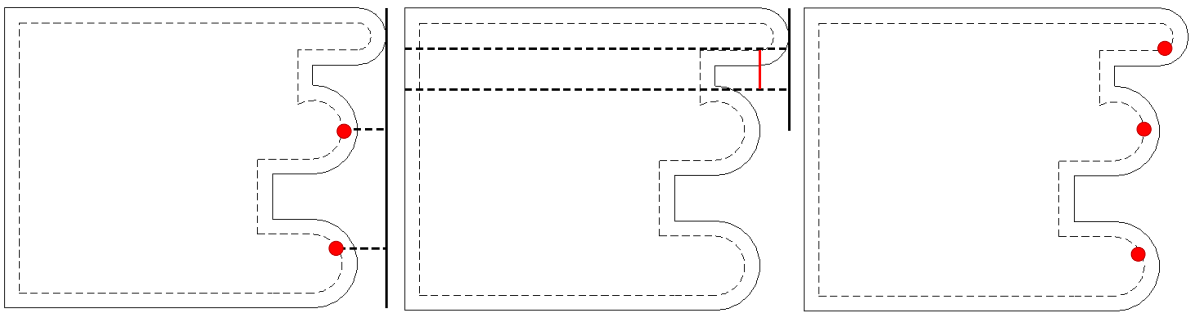

(a) (b) (c)

Figure 38. (a) Defining spans, (b) middle third of largest span and use search line for point closest to the contact edge, (c) place third bolt at this location

Pin Location Algorithm

Dowel pin location follows a different, but similar algorithm to the bolt location algorithm. Figure 39 is an overview of the presented dowel pin location algorithm.

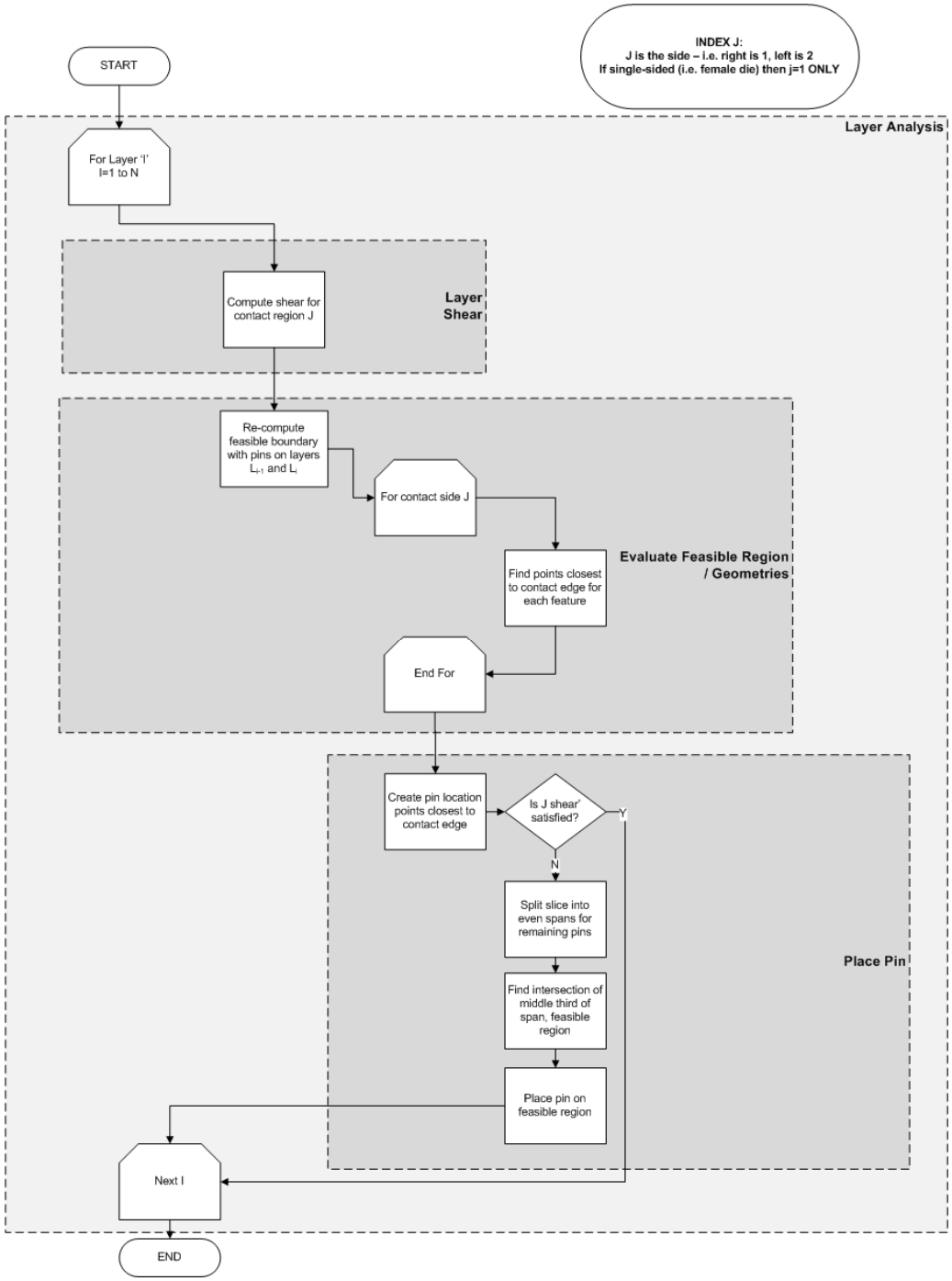

Figure 39. Dowel pin Location Algorithm

The offset boundary is set around previous hardware. Whenever hardware is placed in a slice, an offset equal D_{BZ} or D_{PZ} is placed around the hardware by a Boolean subtraction of a circle from the feasible region. It is important to note that an offset would be placed around the bolt or pin after being placed.

Assuming rigid body, the layer will achieve shear strength when an adequate number of pins are placed between layers. Similar to bolts, pins should be spaced along the geometric feasible space along slice. Ideally, pins should be placed at all major features for proper locating.

However, based on the hardware dimensions and the layer geometry, there may be cases where pins cannot be placed on the desired features. Figure 40 displays a different pin offset boundary. In this case, the top feature cannot contain a pin due to size requirements. In this case, pin locating is lost. Alternatives include using smaller pins or bolts and redesigning the desired geometry.

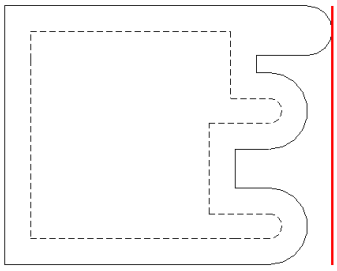

Figure 40. Dowel pin offset boundary for different dowel pin dimensions

Layer Start

Layer start is identical to the bolt location algorithm. The dowel pin algorithm loops for layers 'I' from 1 to N. The largest geometric feasible space occurs at layers first to contact the sheet metal. The algorithm analyzes from the contact layer and continues until no additional layers exist. If no layers exist, the layer analysis can stop looping and the program can terminate.

Within the layer analysis, there are three primary subsections: layer shear, evaluate feasible region/geometries, and place pin. These subsections loop until the layer shear is satisfied.

Layer Shear

If assuming no undercuts, the die has a predetermined amount of dowel pins required for application. The numbers of dowel pins are given in equation 9, $N_p \geq \frac{F_P}{\gamma_{y \cdot (\pi r_p{}^2)}}$. This constitutes the major difference between bolt and pin placement: the number of pins can be easily determined beforehand and is not a function of pin location.

Evaluate Feasible Region/Geometries

Re-compute feasible boundary with pins on layers L_{i-1} and L_i

Similar to the bolt location algorithm, a pin boundary must be determined. The bolt offset boundary was determined based on the slice geometry. The pin feasible region is an offset from the bolt feasible region. If a previous layer contains pins, the offset will be set around the pins.

Find all high points for slice

The algorithm will loop to search for all features for a contact region, J. As previously discussed, a dowel pin is ideally located at every feature. A search line, similar to that used for bolt locating, is used for dowel pin locating. The search line detects peaks.

Create pin location at high points

Creating a dowel pin at the high points along a slice allows the algorithm to satisfy the feature locating dowel pin constraint. A dowel pin is placed on the dowel pin offset boundary at the shortest distance from the point of contact, shown in Figure 41.

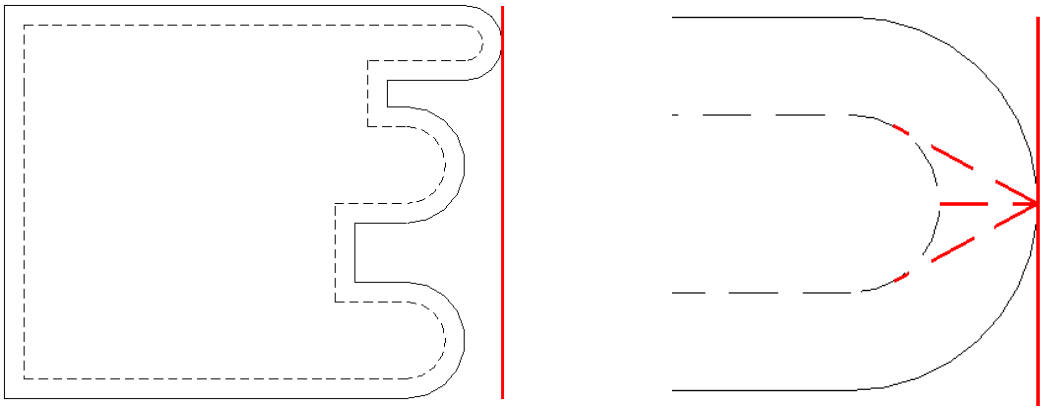

(a) (b)

Figure 41. (a) Point closest to contact edge for dowel pin locating and (b) shortest distance from peak to dowel pin offset boundary

The dowel pins required for each peak loops until all features have been satisfied. A greater number of dowel pins may be placed on the slice if more features exist than dowel pins required for functionality.

Is J 'shear' satisfied?

If all features have been satisfied from above and the required number of dowel pins has been met or surpassed for that given layer, the layer algorithm continues to the next layer.

However, in some cases, more pins may be required than features on the slice. An example of slice geometry with only one feature is shown in Figure 42. Two dowel pins are required at minimum for each layer.

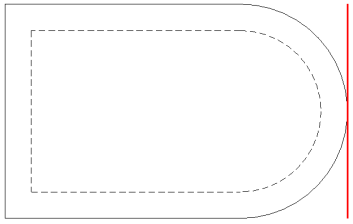

Figure 42. Only one peak with at least two dowel pins required

In this case, the slice is split evenly for the number of dowel pins required for the slice shown in Figure 43.

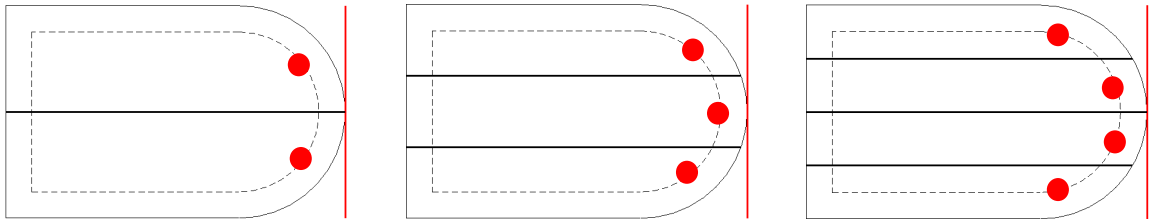

(a) (b) (c)

Figure 43. Evenly spacing dowel pins: (a) two required dowel pins, (b) three required dowel pins, and (c) four required dowel pins

The same principle applies if there is more than one feature, but additional dowel pins are still required. Figure 44 is an example of a two feature slice.

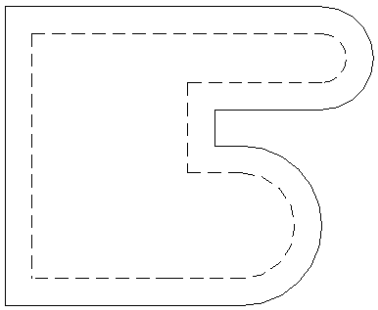

Figure 44. Two feature slice

If three or more dowel pins are required for this slice, the slice is divided into an equal number of spaces. The spaces equal the remaining number of dowel pins. Figure 45 displays the additional dowel pin placement for split dowel pin distances. The red dots represent the dowel pins placed for feature location. The blue dots represent the additional dowel pins placed on the slice.

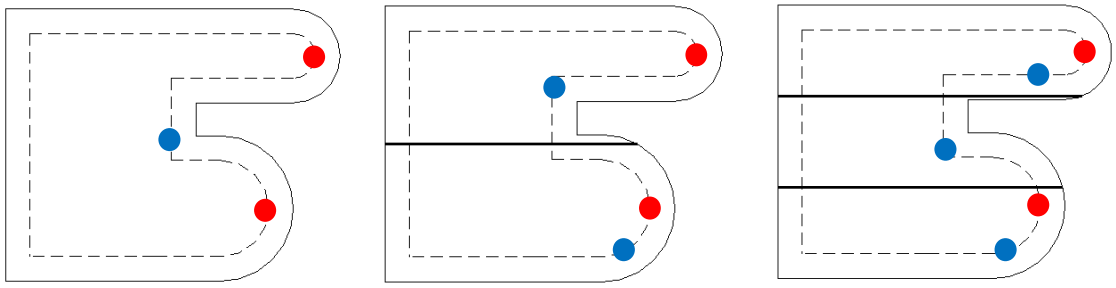

(a) (b) (c)

Figure 45. More than two dowel pins required for two a two feature slice: (a) one additional dowel pin, (b) two additional dowel pins, and (c) three additional dowel pins

Bolt and Dowel Pin Summary

The primary objective of this research is to develop a process planning method for die manufacture, with improved interlaminate stress compared to existing methods. Chapter 4 accomplished the second half of this objective by determining the bolt and dowel pin locations within each slice.

The two sub-objective functions were divided into two different parts with their own constraints: minimize the number of bolts and minimize the number of dowel pins. Mechanical and geometric constraints were determined for each objective function to determine the adequate placement of bolts and dowel pins in each slice.

The expressions for the number of bolts and pins per layer were derived from Chapter 4 and served as an input for the bolt and pin placement algorithm presented in this chapter. Chapter 6 presents a case study of a specific die tooling geometry using the process planning method presented here.

Chapter 6. Case study

Chapter 4 discusses the methodology of determining shear and compressive forces for bending sheet metal. Based on those force components, the number of bolts and pins is determined. Chapter 5 discusses the algorithm for placing the bolts and pins in each layer to withstand adequate forces. This chapter applies the results of Chapters 4 and 5 by presenting a case study for specific die tooling. The case study discusses the steps to complete the previously designed process planning for laminated die manufacture to automatically provide adequate inter-layer strength using a minimum number of fasteners. The specific die tooling considered in this chapter has been designed to incorporate both linear and curved surfaces in a complex manner (i.e. the 'male' die is not entirely convex), shown in Figure 46.

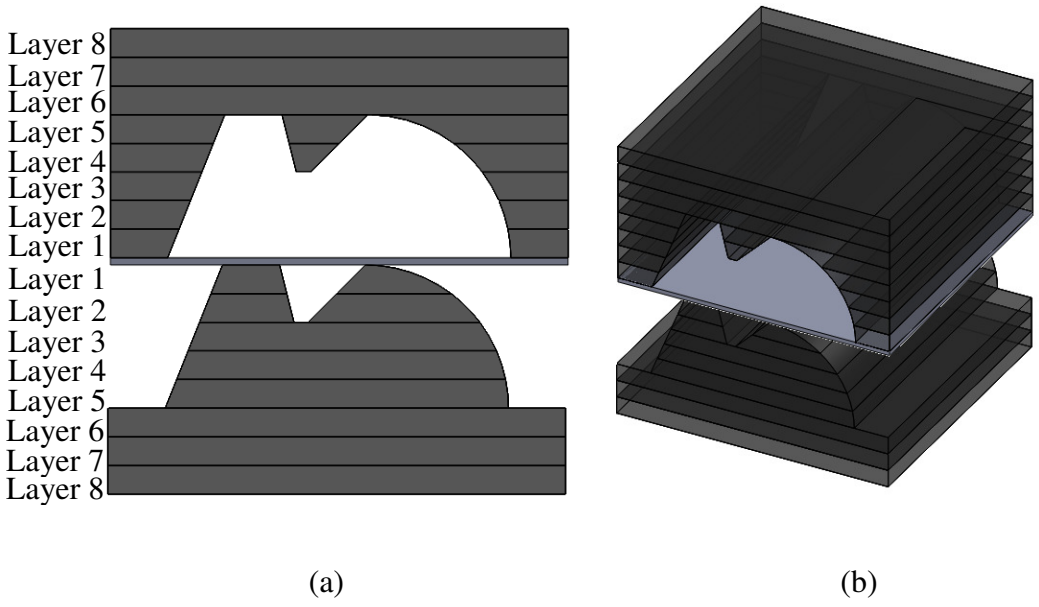

Figure 46. Case study die tooling geometry with eight layers for both female and male halves

The following specifications are assumed:

- Steel plates with 0.5 inch thickness for layers
- Sheet metal thickness of 0.125 inches
- Steel pins with a 0.125 inch diameter

- Steel 6-40 inch bolts

Die Half Contact Forces

As discussed in Chapter 4, the pin force and layer moment equations are based on the die tooling geometry. Figure 47 displays the female die tooling dimensions in unit inches.

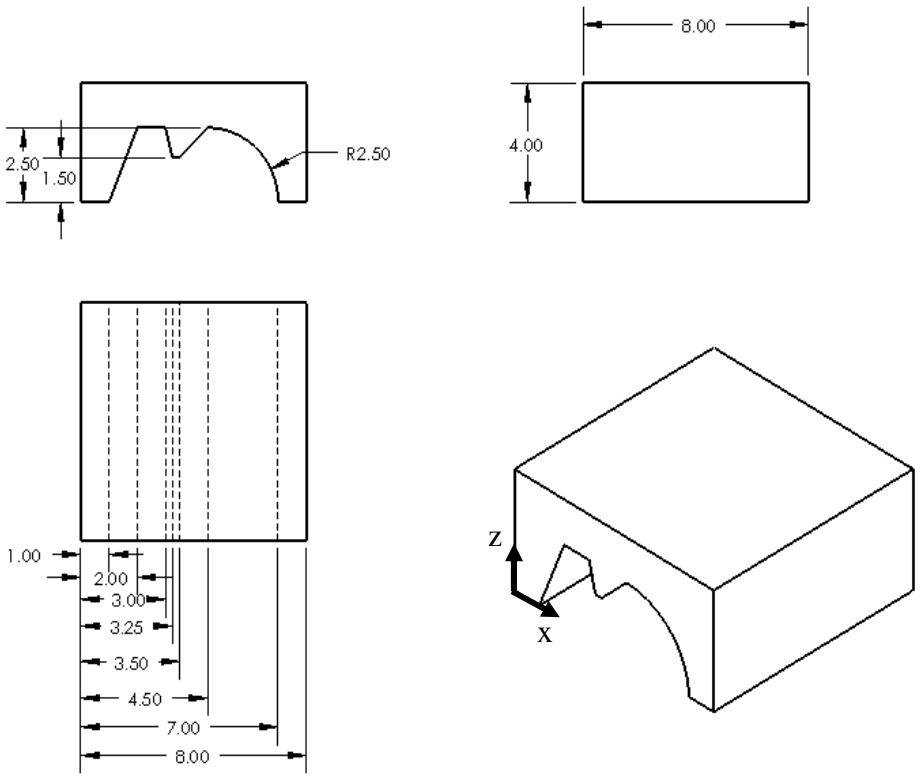

Figure 47. Female die tooling dimensions in inches

Figure 48 displays the male die tooling dimensions in unit inches. The following calculations for pin force are based on both female and male die tooling dimensions.

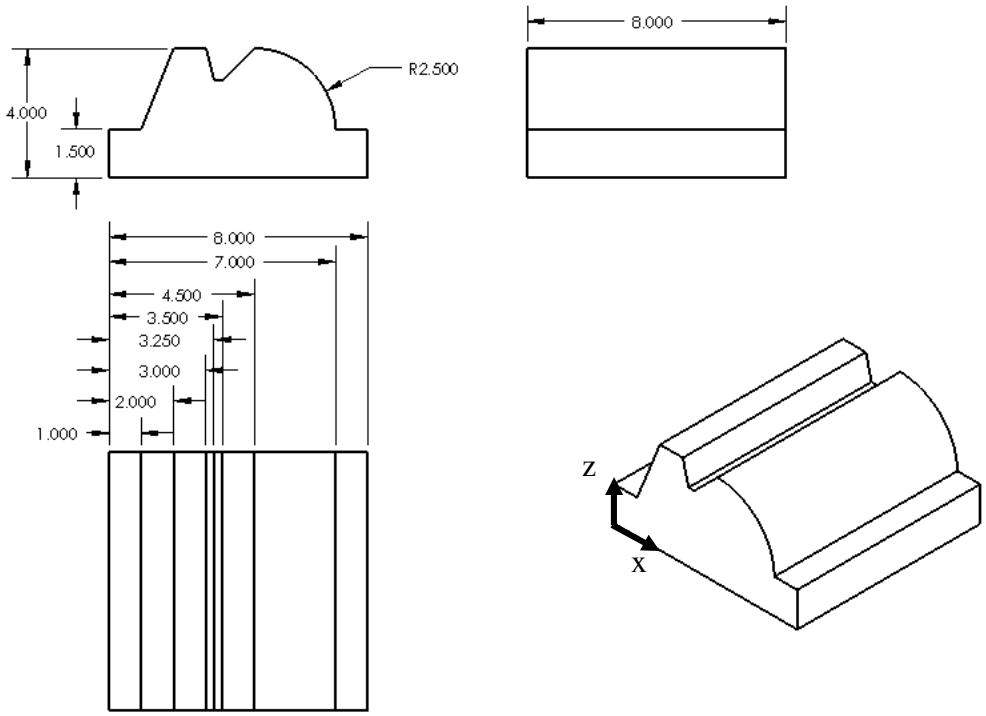

Figure 48. Male die tooling dimensions in inches

Contact Forces

The female die has four contact points, noted by $C_1 – C_4$ in Figure 49a. The contact forces (resultant force, shear force, and compressive force) change over time during sheet metal bending. The number of pins per equation 1, for the male die is the same as the female die given in Table 7. The male die has four contact points similar to the female die, however, C_3 and C_4 are shared by the same point as shown in Figure 49b.

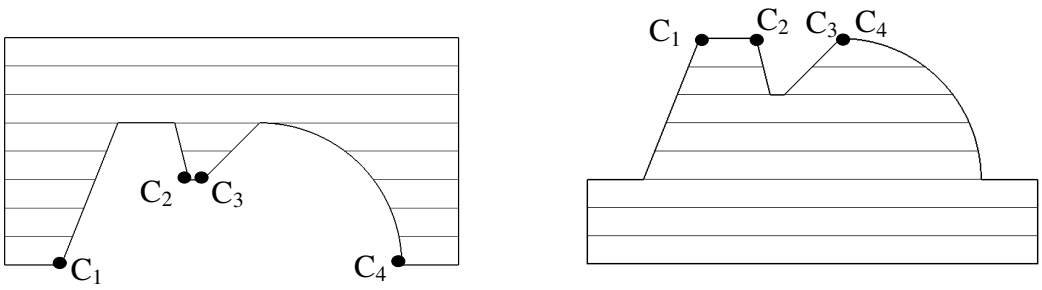

(a) (b)

Figure 49. (a) Female die contact points and (b) male die contact points

The shear force for all contact points is determined below from discussions in Chapter 4. The number of pins can be determined from the maximum pin force for the contact points. As previously mentioned, the force calculations for the four contact points are the same for both female and male dies since the geometry is the same.

Contact Point 1

The moment equation for contact point 1 is plastic because the radius of curvature is very small and is assumed to be a point. The required moment to bend sheet metal given in equation 11 is shown below.

$$M = \frac{\left(95{,}000\ \frac{lb}{in^2}\right)(8\ in)(0.125\ in)^2}{4} = 2{,}970\ lb \cdot in \tag{50}$$

Based on the edge geometry, the maximum pin force occurs at the shutting height, D (from equation 44), shown below where the steel-to-steel coefficient of static friction is 0.74 (Young & Freedman, 2004).

$$D = 2.5\ in - \left(\frac{2.5\ in}{\left(\frac{2.5\ in}{1\ in}\right)}\right)\left(0.74 + \sqrt{0.74^2 + 1}\right) \approx 0.52\ inches \tag{51}$$

Given the sheet metal moment, the maximum pin force for a linear edge to bend sheet metal from equation 43 from contact point 1 is shown below.

$$F_{p(L),max} = (2{,}970\ lb \cdot in)\left(\frac{\left(\frac{2.5\ in}{1\ in}\right)}{2(2.5\ in)}\right)\left(\frac{1}{\sqrt{(0.74)^2+1}+0.74}\right) \approx 749\ lb \quad (52)$$

The forces over time as the sheet metal is bending over the linear edge is given in Figure 50 where F_s is the shear force, F_c is the compressive force, F is the resultant force, and F_P is the force on the pin. The maximum pin force calculated above relates to the bold black line in Figure 50.

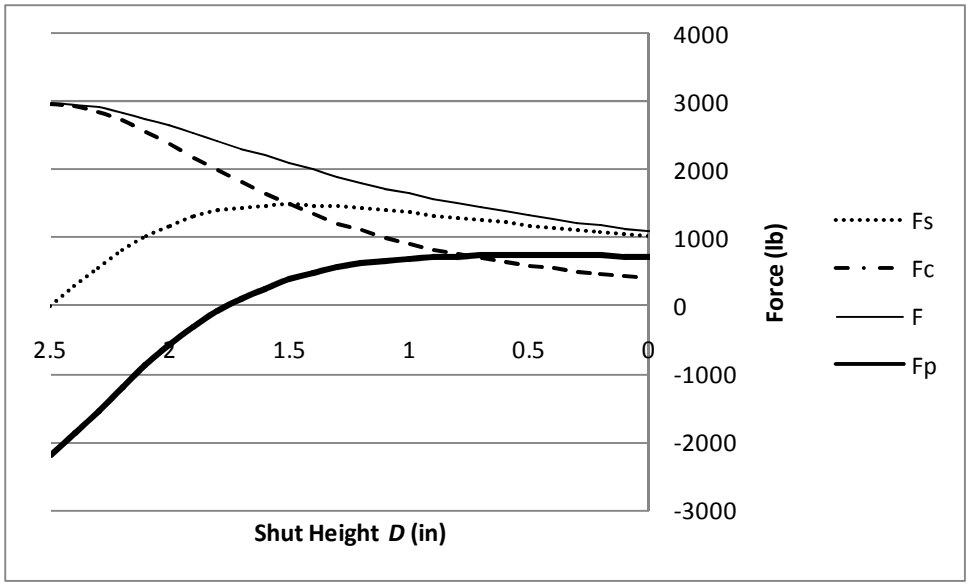

Figure 50. Contact point 1 forces

Contact Point 2

The same bending moment occurs, 2,970 lb·in. Similarly, the maximum pin force occurs at a D value given in equation 53.

$$D = 1\ in - \left(\frac{1\ in}{\left(\frac{1\ in}{2.5\ in}\right)}\right)\left(0.74 + \sqrt{0.74^2 + 1}\right) \approx 0.50\ inches \quad (53)$$

The maximum pin force for contact point 2 is given in equation 54.

$$F_{p(L),max} = (2{,}970\ lb \cdot in)\left(\frac{\left(\frac{1\ in}{1\ in}\right)}{2(1\ in)}\right)\left(\frac{1}{\sqrt{(0.74)^2+1}+0.74}\right) \approx 2{,}947\ lb \quad (54)$$

The forces over time as the sheet metal is bending for contact edge 2 is given in Figure 51 where F_s is the shear force, F_c is the compressive force, F is the resultant force, and F_P is the force on the pin. The maximum pin force calculated above relates to the bolt black line peak in Figure 51.

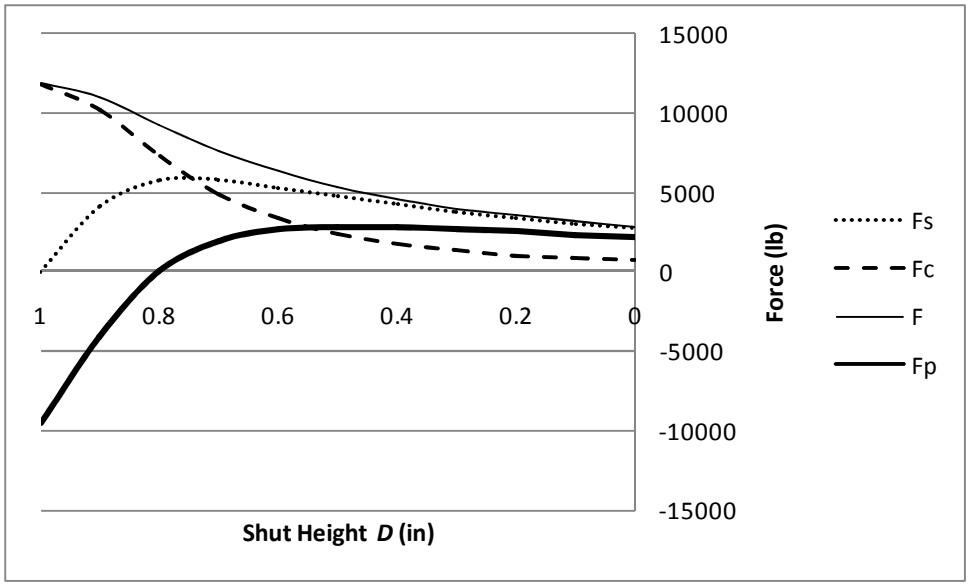

Figure 51. Contact point 2 forces

Contact Point 3

The same bending moment occurs for contact point 3, 2,970 lb·in. The maximum pin force occurs at a D value given in equation 55.

$$D = 1\ in - \left(\frac{1\ in}{\left(\frac{1\ in}{1\ in}\right)}\right)\left(0.74 + \sqrt{0.74^2 + 1}\right) \approx -1.0\ inches \quad (55)$$

Since the die shut height, D, cannot be negative, shear is evaluated when $D = 0$. Therefore, from equation 24, the maximum pin force for contact point 3 is given equation 56.

$$F_{P(L)} = (2{,}970\ lb \cdot in) \cdot \frac{(1-0)-\left(\frac{\frac{1\ in}{\left(\frac{1\ in}{1\ in}\right)}}{1}\right)^{0.74}}{\left(\frac{\frac{1\ in}{\left(\frac{1\ in}{1\ in}\right)}}{1}\right)^{2}+(1-0)^2} \approx 386\ lb \quad (56)$$

The forces for contact point 3 clearly peak when the die is shut (D = 0 inches) shown in Figure 52.

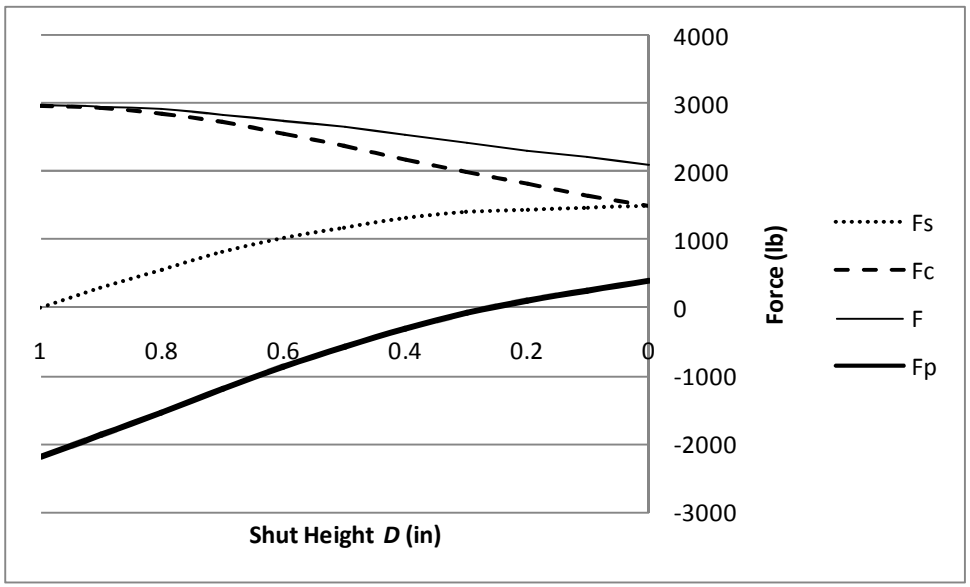

Figure 52. Contact point 3 forces

Contact Point 4

The moment equation for contact point 4 is elastic/plastic because the point is curved. The die tooling is graphed and the minimum of the elastic and plastic moment values were used in the shear force equation (equation 38).

The maximum shear force occurred at the end of the bending. At this point the moment was plastic. The required moment to bend sheet metal is given in equation 11.

$$M = \frac{\left(95{,}000\ \frac{lb}{in^2}\right)(8\ in)(0.125\ in)^2}{4} = 2{,}970\ lb \cdot in \quad (57)$$

The maximum shear force for a linear point to bend sheet metal is given in equation 40.

$$F_{s(P)} = 2{,}970\ \ lb \cdot in \left(\frac{\left(2\sqrt{(2.5\ in)(0.18\ in)} - 2(0.1\ in)\right) - \left(\sqrt{\frac{0.18\ in}{\left(\frac{1}{2.5\ in}\right)}}\right)(0.74)}{\left(2\sqrt{(2.5\ in)(0.18\ in)} - 2(0.18\ in)\right)^2 + \left(\sqrt{\frac{0.18\ in}{\left(\frac{1}{2.5\ in}\right)}}\right)^2} \right) \approx 1{,}019\ lb \tag{58}$$

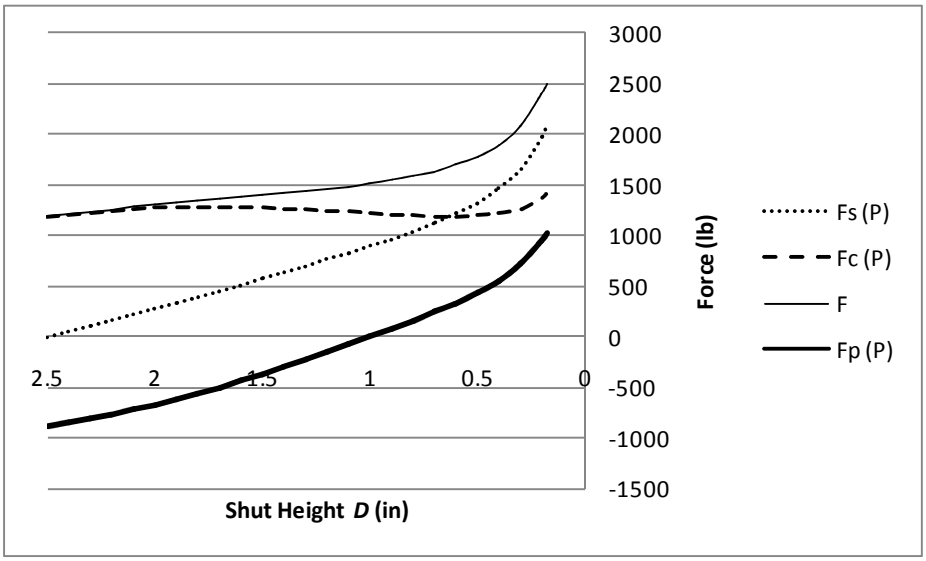

Figure 53. Contact point 4 forces

Moment Calculations

The first step in the bolt location algorithm in Figure 29 is to calculate the layer moments. The maximum layer moment is determined by maximizing D give the layer height, h, and the width, w. The female die has eight layers, but only seven layer interfaces for hardware placement. Figure 54 displays a few of these intersections.

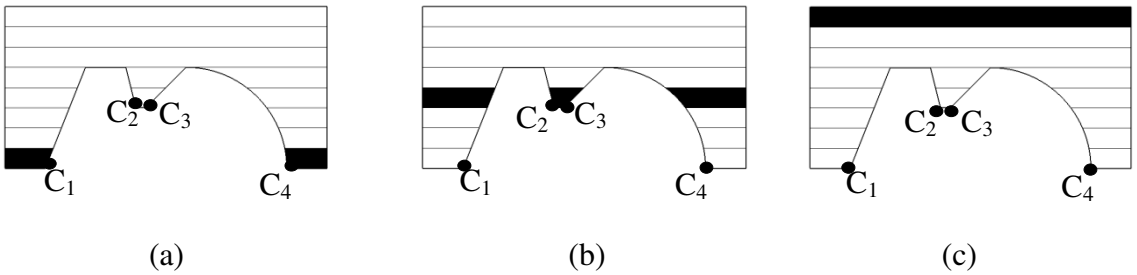

Figure 54. Female die layer 1 (a), layer 4 (b), and layer 8 (c)

Maximizing D for linear surface shear and compressive forces (equations 24 and 25) and parabolic surface shear and compressive forces (equations 38 and 39) were calculated by using the maximize function of goal seek in Microsoft Excel. Female layer moment calculations for each layer are summarized in Table 1 in units of lb·in. Extensive layer moment calculations are provided Appendix II. Moment Calculations for Female Die.

Table 1. Female die moment calculations for each layer (lb·in)

	Contact Point 1	Contact Point 2	Contact Point 3	Contact Point 4
Layer 1	102.4	-	-	-398.7
Layer 2	614.8	-	-	810.1
Layer 3	1191.6	-	-	2018.8
Layer 4	1834.8	898.9	-44.8	3227.5
Layer 5	2512.4	2082.8	281.5	4436.3
Layer 6	3209.6	873.2	-3659.8	5645.0
Layer 7	3918.8	2270.2	-3147.9	6853.7

If the moment layer is negative, a moment does not exist. However, a bolt must still be placed at the interface between the two layers. The bolt force must withstand the mass of the current layer and the previous layers. An overview of layer the mass for each contact point, calculated from equation 2, is provided in Table 2 where the density of steel is 0.284 $\frac{lb}{in^3}$ (Groover, 2002).

Table 2. Female die layer mass (lb)

	Contact Point 1	Contact Point 2	Contact Point 3	Contact Point 4
Layer 1	1.24	-	-	1.15
Layer 2	1.47	-	-	1.26
Layer 3	1.69	-	-	1.51
Layer 4	1.92	0.63		1.95
Layer 5	2.14	1.34		2.79
Layer 6	9.02			
Layer 7	9.02			
Layer 8	9.02			

The male die has eight layers with seven layer interfaces for hardware placement. Figure 55 displays the layer sequence for the male die.

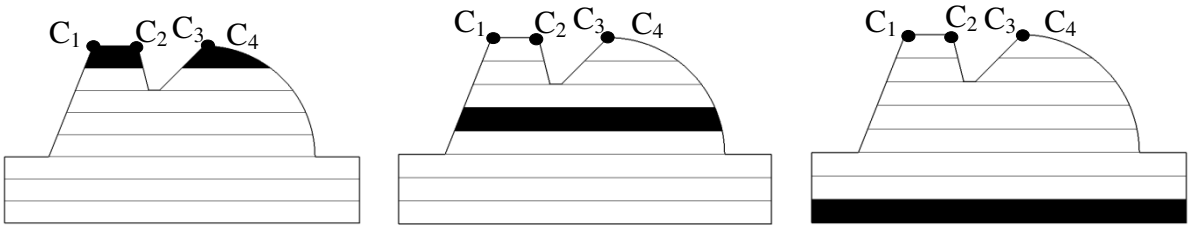

(a) (b) (c)

Figure 55. Male die layer 1 (a), layer 4 (b), and layer 8 (c)

Male layer moment calculations for each layer are summarized in Table 3 in units of lb·in. The same process as the female die is used for determining the maximum layer moment. Extensive layer moment calculations are provided in Appendix V. Moment Calculations for Male Die.

Table 3. Male die layer moment calculations for each layer (lb·in)

	Contact Point 1	Contact Point 2	Contact Point 3	Contact Point 4
Layer 1	1.31		1.43	
Layer 2	1.68		2.84	
Layer 3	5.81			
Layer 4	6.29			
Layer 5	6.63			
Layer 6	9.02			
Layer 7	9.02			
Layer 8	9.02			

Similar to the female die, the male die has negative moments for particular contact points. Therefore, the mass of that layer and the previous layers must be considered for bolt placement. The mass for the male die layers is given in Table 4.

Table 4. Male die layer mass (lb)

	Contact Point 1	Contact Point 2	Contact Point 3	Contact Point 4
Layer 1	1.31		1.43	
Layer 2	1.68		2.84	
Layer 3	5.81			
Layer 4	6.29			
Layer 5	6.63			
Layer 6	9.02			
Layer 7	9.02			
Layer 8	9.02			

Bolt and Pin Algorithm

The bolt used is a standard #6-40 inch stainless steel bolt with a head diameter of 0.226 inches. Stainless steel material for bolts is arbitrary. The user can input any bolt material type. All bolt offsets are one bolt head diameter. Bolt dimensions were obtained from McMaster-Carr.com (Socket Cap Screws). The total offset from the center point of the bolt is 0.339 inches. First, the shear area, stiffness, and preload force of the bolt are determined.

$$A_s = \frac{\pi}{4}\left[0.112\ in - \left(\frac{0.9745}{40}\right)\right]^2 = 0.01\ in^2 \tag{59}$$

$$K_B = \frac{\left(30{,}000{,}000\,\frac{lb}{in^2}\right)(0.01\,in^2)}{0.25\,in} \approx 723{,}854\,\frac{lb}{in} \tag{60}$$

$$F_{PRELOAD} = 723{,}834\,\frac{lb}{in} \cdot 0.025\,in \cdot \frac{60}{360} \approx 3{,}016\,lb \tag{61}$$

Equations 59, 60, and 61 are inputs for the bolt force.

$$F_B = \frac{\left(95{,}000\,\frac{lb}{in^2} - 3{,}016\,lb\right)(0.01\,in^2)}{1.5} \approx 369.9\,lb \tag{62}$$

Bolt and Pin Locating Tool

Chapter 5 discusses the bolt and pin placement requirements. However, the bolt and pin locating tool is not a deliverable of these requirements.

The program simply provides an exact bolt or pin location to reduce error in determining this location. The locating tool is pre-existing code that determines the feasible boundary, the intersection of span with feasible region, and the high points in feasible span. The inputs are the STL file, slice height, offset value, span location, previous bolt and dowel pin coordinates, and D_{BZ} and D_{PZ} values. The program outputs a single coordinate at the high point. Figure 56 displays a trimetric view of the STL female and male dies with their associated origin in the program. The program is simply a tool for determining bolt and dowel pin coordinates.

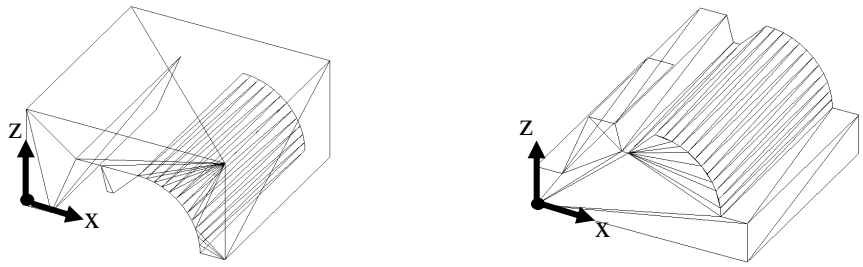

(a) (b)

Figure 56. STL file with origin of female die (a) and male die (b)

Sample Calculation: Female Die Layer 4, Contact Point 1

The moment calculations for the female and male die tooling were previously determined. The second part (Evaluate Feasible Region/Constraints) and third part (Place Bolt) of the bolt locating algorithm in Figure 29 is dependent on the slice geometry. The input from the first part of the bolt locating algorithm for contact point 1 is the shear and compressive forces for layer 4 are shown in Figure 57.

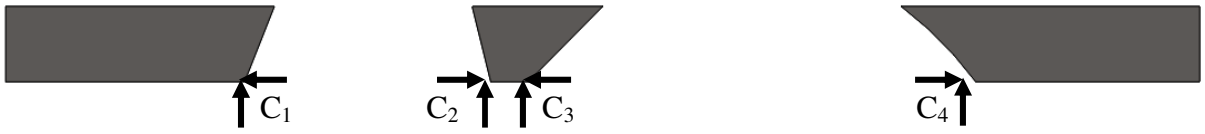

Figure 57. Layer 4 of female die

The layer moment is the mechanical constraint for the initial algorithm loop for contact point 1. The layer moment for contact point 1 is 1,834.8 lb·in from Table 1. The constraints are not satisfied since a bolt has not been placed on this layer. Using the location program discussed earlier, the offsets for the bolts in L_{i-1} (Layer 3) have been subtracted from the current layer shown in Figure 58. If multiple contact points existed on this layer, the largest layer moment would be evaluated first. However, in this case, there is only one contact point to evaluate, therefore, contact point.

When placing the bolt, the largest span is first evaluated. The span in the y axis for this case is (0 inches, 8 inches). Contact point 1 is along the lower gray edge of Figure 58. The feasible region exists, therefore the highest point is chosen to maximize the layer moment. The maximum distance in the x axis is chosen. The first bolt will be placed on the feasible region in the middle third of the slice. Therefore, the bottom blue dot is chosen for the first bolt.

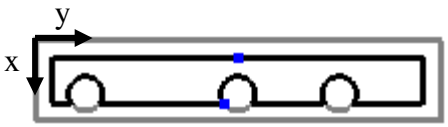

Figure 58. Contact point 1 bolt location for span 0 inches to 8 inches

The bolt locating algorithm loops back to compute mechanical constraints. Equation 63 displays the layer moment resistance from one bolt. The mechanical constraints are not satisfied and a second bolt must be placed on the layer.

$$M_{L_i} = 1834.8 \text{ lb} \cdot \text{in} \leq 369.9\ lb \cdot 1.261\ in \approx 466.4\ lb \cdot \text{in} \quad (63)$$

The first bolt and its offset region are placed. The first span split occurs. The y ranges are (0 inches, 3.72657 inches) and (3.72657 inches, 8 inches). The largest range is (3.72657 inches, 8 inches), therefore, the second bolt will search in the middle third of this region.

Figure 59. Contact point 1 bolt location for span 3.72657 inches to 8 inches

The bolt locating algorithm loops to compute mechanical constraints. Equation 64 displays the layer moment resistance from the second bolt. The mechanical constraints are not satisfied and a third bolt must be placed on the layer.

$$M_{L_i} = 1834.8 \text{ lb} \cdot \text{in} \leq 369.9\ lb \cdot (1.261\ in + 1.261\ in) \approx 932.9\ lb \cdot \text{in} \quad (64)$$

The second bolt and its offset region are placed in the slice. The second span split occurs. The y ranges are (0 inches, 3.72657 inches), (3.72657 inches, 5.72657 inches), and (5.72657 inches, 8 inches). The largest range is (0 inches, 3.72657 inches), therefore the third bolt will search in the middle third of this region.

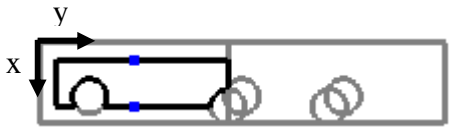

Figure 60. Contact point 1 bolt location for span 0 inches to 3.72657 inches

The bolt locating algorithm loops to compute mechanical constraints. Equation 65 displays the layer moment resistance from the third bolt. The mechanical constraints are not satisfied and a fourth bolt must be placed on the layer

$$M_{L_i} = 1834.8 \text{ lb} \cdot \text{in} \leq 369.9\ lb \cdot (1.261\ in + 1.261\ in + 1.261\ in) \approx 1399.3\ lb \cdot \text{in} \quad (65)$$

The third bolt and its offset region are placed in the slice. The third span split occurs. The y ranges are (0 inches, 1.86329 inches), (1.86329 inches, 3.72657 inches), (3.72657 inches, 5.72657 inches), and (5.72657 inches, 8 inches). The largest range is (5.72657 inches, 8 inches); therefore the third bolt will search in the middle third of this region.

Figure 61. Contact point 1 bolt location for span 5.72657 inches to 8 inches

The bolt locating algorithm loops to compute mechanical constraints. Equation 66 displays the layer moment resistance from the fourth bolt. The mechanical constraints are satisfied and the program ends for layer 4.

$$M_{L_i} = 1834.8 \text{ lb} \cdot \text{in} \leq 369.9\ lb \cdot (1.261\ in + 1.261\ in + 1.261\ in + 1.261\ in) \approx 1865.8\ lb \cdot \text{in} \quad (66)$$

Bolt locations for the female die are summarized in Appendix III. Bolt Locations for Female Die. Bolt locations for the male die are summarized in Appendix VI. Bolt Locations for Male Die. The total number of bolts to satisfy the layer moment conditions for the female die is given in Table 5.

Table 5. Number of bolts for female die

	Bolt Summary			
	C1	C2	C4	Total per layer
Layer 1	1	-	1	2
Layer 2	2	-	3	5
Layer 3	4	-	6	10
Layer 4	4	6	9	19
Layer 5	4	9	8	21
Layer 6	2	-	2	4
Layer 7	2	-	3	5
Total Bolts				66

The total number of bolts to satisfy the layer moment conditions for the male die is given in Table 6.

Table 6. Number of bolts for male die

	Bolts per Layer		
	C2	C4	Total per layer
Layer 1	2	1	3
Layer 2	6	1	7
Layer 3	2	-	2
Layer 5	4	-	4
Layer 6	3	-	3
Layer 7	4	-	4
Total Bolts			23

The number of bolts would change for the same die geometry based upon the bolt material. In this case, stainless steel bolts were arbitrarily chosen. A bolt material with a higher tensile strength, E, would reduce the number of bolts for each die half for the given geometry. This is simply an example of the die tooling design to resist delamination from bending forces.

Number of Pins

Per equation 1, assuming a pin safety factor of 1.25, a summary of pins for the given contact point geometry is given in Table 7. This applies to both the female and male die halves since the geometry is the inverse of one another.

Table 7. Contact points number of pins

	Number of Pins
Contact Point 1	2
Contact Point 2	6
Contact Point 3	2
Contact Point 4	2

Female Die Counteracting Pin Forces

The pin forces previously calculated were for each independent contact point. However, in reality, there are two sides to each layer. Pin force may occur only on either contact point.

The female die has one case of counteracting pin forces. Contact points 2 and 3 have counteracting pin forces as shown in Figure 62. To conservatively estimate the number of pins required for counteracting pin forces, the number of pins calculated for each contact point are summed together. In this case, contact point 2 requires six pins and contact point 3 requires two pins, therefore, eight pins are required.

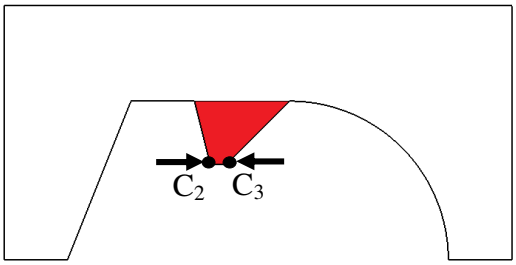

Figure 62. Counteracting shear forces on C_2 and C_3

Male Die Counteracting Shear Forces

Using the same principles as shown for the female die, the total number of pins used is the sum of pins from each contact point. For instance, the direction of shear forces for C_1 and C_2 in Figure 63. C_1 requires two pins and C_2 requires six pins, therefore, eight pins are used for each layer.

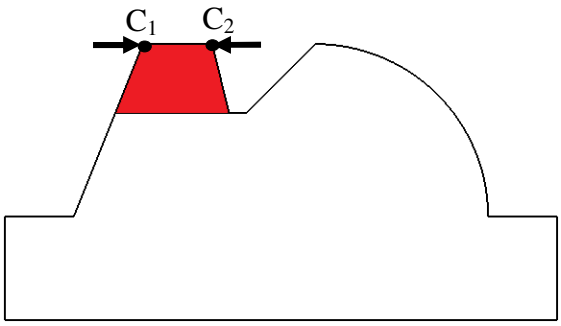

Figure 63. Counteracting shear forces on C_1 and C_2 for the male die

Similarly, the counteracting moment between contact points C_3 and C_4 occur in layers 1 and 2. C_3 requires two pins and C_4 requires two pins. Therefore, four pins will be used for each layer.

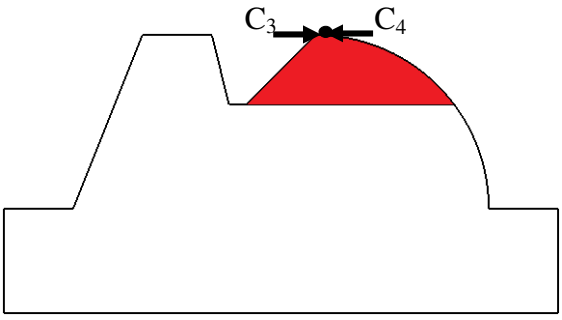

Figure 64. Counteracting shear forces on C_3 and C_4 for the male die

Lastly, the counteracting moment acting on the male die occurs on layers 3 – 5 between contact points C_1 and C_4 result in a total of four pins.

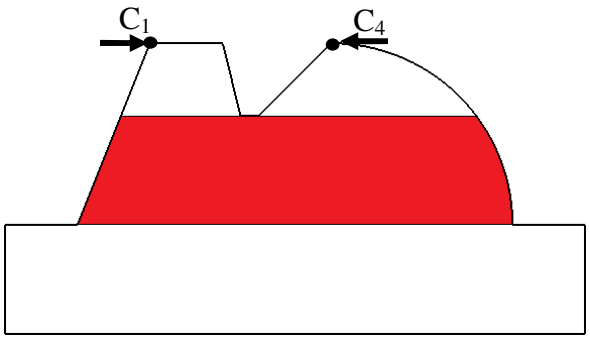

Figure 65. Counteracting shear forces on C_1 and C_4 for the male die

Once all bolt locations are determined, the pin locations will be determined. Using layer 4, contact point 1, two pins are required for this layer. Therefore, from Chapter 5, the layer will be divided into two halves. The pins will be placed on either the maximum or the minimum location on the x axis. Bolts from layers 3, 4, and 5 are viewed for feasible regions. The first pin is placed at location (0.339, 2.1875).

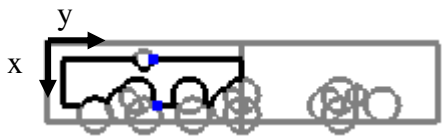

Figure 66. Contact point 1 pin location for span 0 inches to 4 inches

The span is split from 4 inches to 8 inches to determine the feasible location for the second pin. Figure 67 displays two feasible locations for the second pin. The second pin is placed at location (1.261, 6.2743).

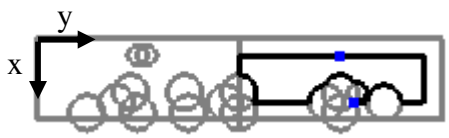

Figure 67. Contact point 1 pin location for span 4 inches to 8 inches

Using the bolt locations in Appendix III and Appendix VI and dowel pin locations in Appendix IV and Appendix VII, the female and male die halves can be assembled. Figure 68 displays layer 5 and layer 6 from the female die with proper bolt and dowel pin locations. Figure 69 displays layer 5 and layer 6 from the female die assembled together.

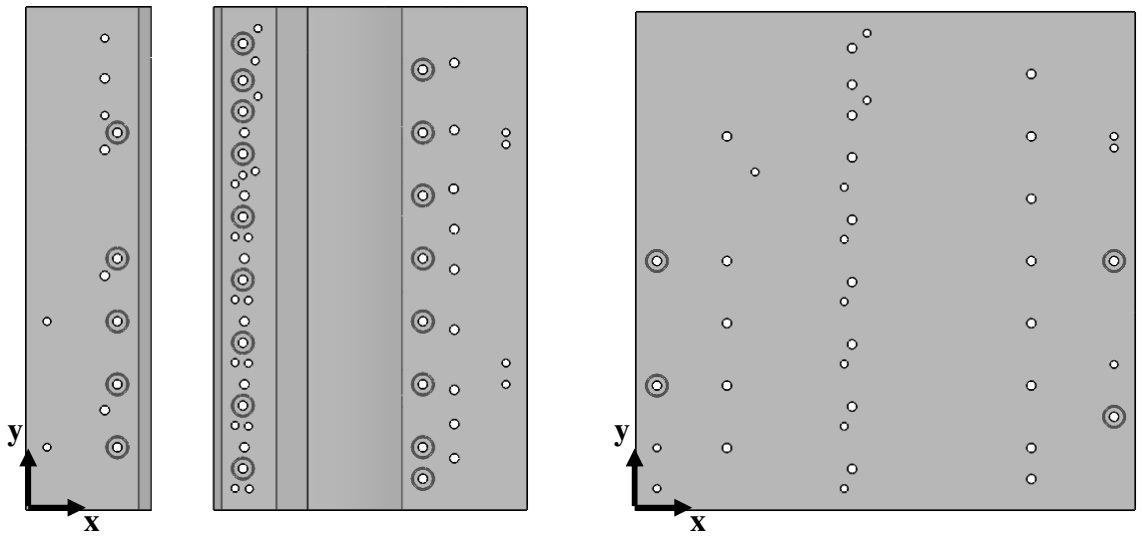

Figure 68. (a) Female die layer 5 bolt and dowel pin locations and (b) female die layer 6 bolt and dowel pin locations

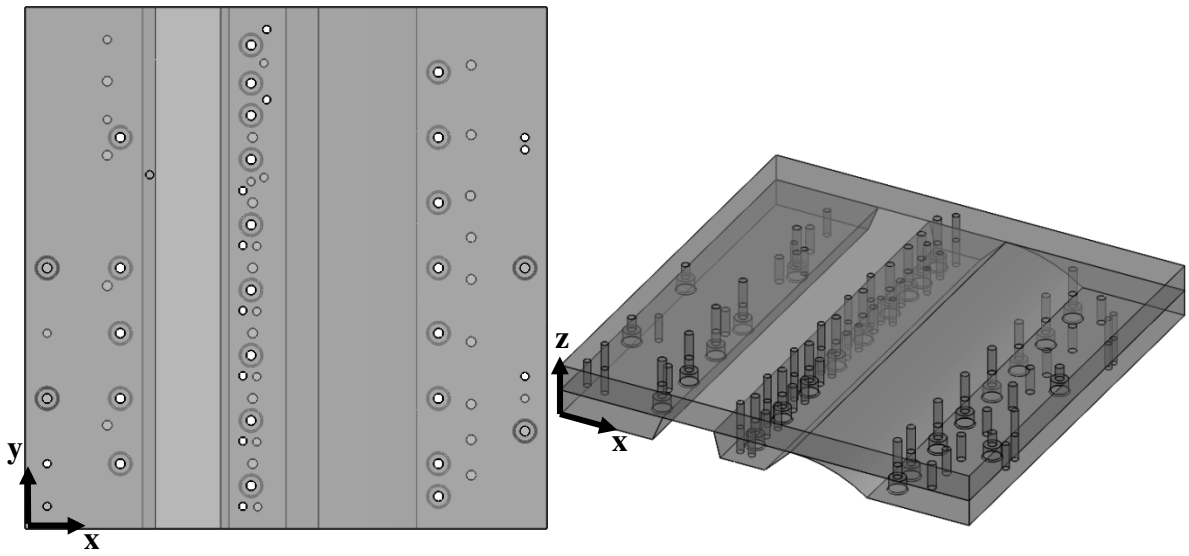

Figure 69. Female die layer 5 and layer 6 bolted together

Case Study Summary

The bolt and pin placement algorithm is not an optimization algorithm, rather a heuristic method for placing bolts and pins to achieve adequate interlaminate strength. The case study

presented in Chapter 6 stepped through the process planning for one particular die tooling. Based on the die tooling geometry, the pin force and the layer moment were determined. The quantity and placement of bolts was determined based upon the bolt location algorithm introduced in Chapter 5. The final female and male die tooling with proper bolt and dowel pin locations are shown in Figure 70 and Figure 71.

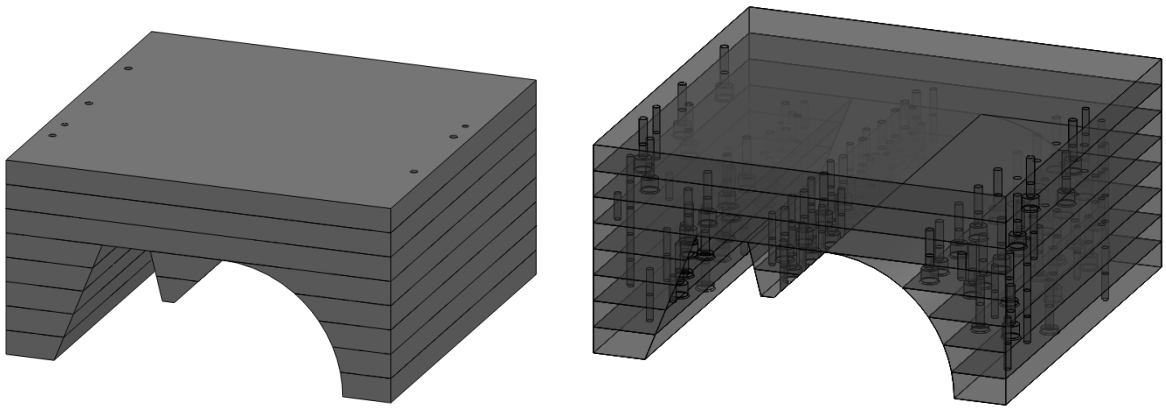

(a) (b)

Figure 70. (a) Solid female die with bolts and dowel pins and (b) transparent view of bolts and dowel pins

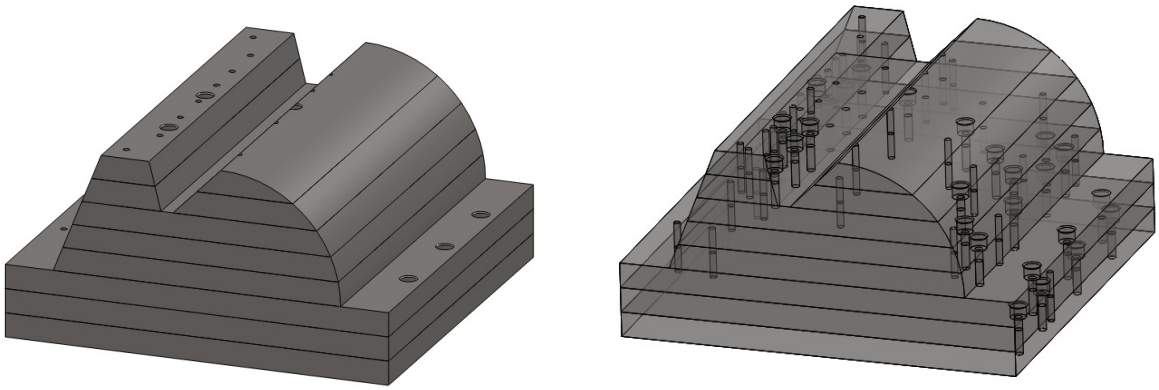

(a) (b)

Figure 71. (a) Solid male die with bolts and dowel pins and (b) transparent view of bolts and dowel pins

The number of pins was determined from the methodology introduced in Chapter 3 and the pin force introduced in Chapter 4. The pin location algorithm from Chapter 5 was utilized for the die tooling in Chapter 6.

Chapter 7. Discussion

The application of rapid die tooling branches from the excessive lead time for adequate design and tooling repair. From Walczyk's work (Walczyk & Hardt, 1998), laminated die tooling requires four essential elements: (1) automation, (2) layer registration, (3) securing for tool rigidity, and (4) disassembly. This thesis presents a process planning method to automatically provide adequate interlaminate strength using a minimum number of fasteners.

The proposed process planning inputs die geometry, predetermined layer thickness, die material properties, predetermined hardware size, and sheet metal properties. The algorithms provided by this research output specific bolt and dowel pin locations for adequate interlaminate strength. Specific locations for bolts and dowel pins accomplish elements 2 and 3 of Walczyk's four essential elements for rapid die tooling.

The quantity and location of bolts and dowel pins is relatively simple, as explained in Chapter 3. One contribution of this thesis is solving for the mechanical requirements to bend sheet metal by predicting the shear and compressive forces on laminated tooling. Methods existed to predict compressive forces for sheet metal bending. However, a model to predict shear and compressive forces for a given die tooling geometry as a function of shut height did not exist prior to this research.

Using the general shear and compressive force equations, forces for linear and parabolic die tooling geometries were adapted. Maximum pin force was derived for linear geometry by use of the first derivative test. For a parabolic surface, a graphical approach was taken to find the maximum pin force by varying input parameters A and C.

Boothroyd's energy model of bending sheet metal was compared to the proposed method of bending sheet metal. Boothroyd's output was average compressive force. For the given input geometry, Boothroyd's method determined an average compressive force of 3,800 lb, whereas the proposed model outputted an average compressive force of 5,024 lb. The variability in the compressive force results can be attributed to the proposed force model fitting a parabolic surface to a curved surface. Furthermore, the proposed model is

conservative in force predictions. Future work can experimentally measure the magnitude of shear and compressive forces during sheet metal bending.

Upon determining the shear and compressive forces for the inputted die geometry, bolt and dowel pin location algorithms were developed. The bolt location algorithm was developed to determine the number and location of bolts for each interlaminate surface. The dowel pin location algorithm determines their location for each interlaminate surface. Since bolt location is an input to satisfying the layer moment mechanical requirement, the bolt location algorithm is conducted first. Dowel pin locating performs layer registration as well as resists interlaminate shear force. The dowel pin location algorithm searches for slice peaks and places a pin at the nearest feasible region. Future work includes computer implementation of both the bolt and dowel pin location algorithms.

A case study described the process planning method for die tooling. The design used relatively thick sheet metal (0.125 inch thick) to demonstrate the high shear and compressive forces acting on the layers. Small fasteners were used to display scalability of die tooling; a larger die would use correspondingly larger fasteners. Future work in this area includes comparing the tool life laminated dies with that of solid die tooling.

The research presented in this thesis provides as a method of shortening the time period from design to manufacturing of die tooling. Future work in the sheet metal bending area for rapid die tooling includes adaptive layer registration. The current model only applies to die tooling with geometry heights at multiples of the layer thickness. This is not always convenient in practice. Also, this model assumes only one bolt and one dowel pin size is used. In some cases, it may be useful to have a variety of bolt and dowel pin sizes. Future work in the surface geometries for force analysis can be studied as well as surface geometry identification. Lastly, the presented work can be adapted to other applications for rapid manufacturing where layer disassembly is a requirement. Other mechanical applications of this method could include punch and drawing dies, lost foam molds, thermoforming molds, and fixtures.

Works Cited

Akula, S., & Karunakaran, K. (2006). Hybrid adaptive layer manufacturing: An Intelligent art of direct metal rapid tooling process. *Robotics and Computer-Integrated Manufacturing* , 113-123.

Bickford, J. H. (2008). *Introduction to the Design and Behavior of Bolted Joints (Fourth Edition).* Boca Raton: CRC Press.

Boonsuk, W., & Frank, M. C. (2009). Automated fixture design for a rapid machining process. *Rapid Prototyping Journal* , 111-125.

Boothroyd, G., Knight, W., & Dewhurst, P. (2002). *Product Design for Manufacture & Assembly.* New York: Marcel Dekker, Inc.

Clevenger, W. S., Cohen, J. S., & Cohen, S. G. (1954). *Patent No. 2679172.* United States of America.

DiMatteo. (1976). *Patent No. 3932923.* United States of America.

Du, Z. H., Chua, C. K., Chua, Y. S., Loh-Lee, K. G., & Lim, S. T. (2002). Rapid Sheet Metal Manufacturing. Part 1: Indirect Rapid Tooling. *Advanced Manufacturing Technology* , 411-417.

Groover, M. P. (2002). *Fundamentals of Modern Manufacturing.* New York: John Wiley & Sons, Inc.

Hart, F. V. (1942). *Patent No. 2274060.* United States of America.

Hosford, W. F., & Caddell, R. M. (2007). *Metal Forming: Mechanics and Metallurgy (Third Edition).* New York: Cambridge University Press.

Im, Y.-T., & Walcyzk, D. F. (2002). Development of a Computer-Aided Manufacturing System for Profiled Edge Lamination Tooling. *American Society of Mechanical Engineers* , 754-761.

Metals, A. S. (1982). *Tool and Die Failures Source Book.* Metals Park: American Society for Metals.

Shigley, J. E. (1956). *Machine Design.* York: The Maple Press Company.

Shook, J. T., & Walczyk, D. F. (2004). Structural Modeling of Profield Edge Laminate (PEL) Tools Using the Finite Element Method. *American Society of Mechanical Engineers* , 64-73.

Socket Cap Screws. (n.d.). Retrieved April 25, 2010, from McMaster-Carr: http://www.mcmaster.com/#socket-cap-screws/=6tjctf

Stewart, J. (2009). *Calculus.* Belmont: Tomson Corporation.

Walczyk, D. F., & Hardt, D. E. (1999). A Comparison of Rapid Fabrication Methods for Sheet Metal Forming Dies. *American Society of Mechanical Engineers* , 214-224.

Walczyk, D. F., & Hardt, D. E. (1998). Rapid Tooling for Sheet Metal Forming Using Profiled Edge Laminations - Design Principle and Demonstration. *American Society of Mechanical Engineers* , 746-754.

Walczyk, D. F., & Hardt, D. E. (1998). Rapid Tooling for Sheet Metal Forming Using Profiled Edge Laminations - Design Princples and Demonstration. *ASME* , 746-754.

Walczyk, D. F., & Im, Y.-T. (2005). Structural Modeling of Profiled Edge Laminae (PEL) Tools. *Journal of Manufacturing Science and Engineering* , 138-147.

Walczyk, D. F., & Yoo, S. (2009). Design and fabrication of a laminated thermoforming tool with enhanced features. *Journal of Manufacturing Processes* , 8-18.

Yoo, S., & Walczyk, D. (2005). An advanced cutting trajectory algorithm for laminated tooling. *Rapid Prototyping Journal* , 199-213.

Young, & Freedman. (2004). *University Physics with Modern Physics 11th Edition.* San Francisco: Pearson Education, Inc.

Appendix I. First Derivative Test: Linear Surface

The function, pin force over die shutting distance, is derived for the point in which the slope is zero.

$$\frac{dF_{P(L)}}{dD} = 0 \tag{67}$$

The first derivative of the total pin force is evaluated in equation 68.

$$\frac{\mathrm{dF_{P(L)}}}{\mathrm{dD}} = M\frac{\mathrm{d}}{\mathrm{dD}}\left(\frac{(C-D)-\mu\left(\frac{C}{A}\right)}{\left(\frac{C}{A}\right)^2+(C-D)^2}\right) \tag{68}$$

Using the chain rule, equation 68 can be expanded into equation 69.

$$\frac{\mathrm{dF_{P(L)}}}{\mathrm{dD}} = M\left[\frac{1}{\left(\frac{C}{A}\right)^2+(C-D)^2}\frac{d}{dD}\left((C-D)-\mu\left(\frac{C}{A}\right)\right)+\left((C-D)-\left(\frac{C}{A}\right)\mu\right)\frac{d}{dD}\left(\frac{1}{\left(\frac{C}{A}\right)^2+(C-D)^2}\right)\right] \tag{69}$$

The first derivative of equation 69 is calculated and set equal to zero to determine the local maximum pin force shown in equation 70.

$$\frac{\mathrm{dF_{P(L)}}}{\mathrm{dD}} = M\left[\left(\frac{-1}{\left(\frac{C}{A}\right)^2+(C-D)^2}\right)\left(1-\left(\frac{2(C-D)\left((C-D)-\left(\frac{C}{A}\right)\mu\right)}{\left(\frac{C}{A}\right)^2+(C-D)^2}\right)\right)\right] = 0 \tag{70}$$

Further reducing of equation 70, can be evaluated into equation 71 below.

$$\frac{\mathrm{dF_{P(L)}}}{\mathrm{dD}} = 1-\left(\frac{2(C-D)\left((C-D)-\left(\frac{C}{A}\right)\mu\right)}{\left(\frac{C}{A}\right)^2+(C-D)^2}\right) = 0 \tag{71}$$

A quadratic expression can be derived from equation 71, shown in equation 72.

$$(C-D)^2 - 2\mu\left(\frac{C}{A}\right)(C-D) - \left(\frac{C}{A}\right)^2 = 0 \tag{72}$$

Solving for $(C-D)$ in equation 72 and subsequently C, one obtains the position D of maximum pin force:

$$D = C - \left(\frac{C}{A}\right)\left(\mu \pm \sqrt{\mu^2+1}\right) \tag{73}$$

Since D must be in the range [0,C], the final expression is give in equation 74.

$$D = C - \left(\frac{C}{A}\right)\left(\mu + \sqrt{\mu^2+1}\right) \tag{74}$$

As μ (dependent on the sheet metal and die material) approaches zero, $D = C - \left(\frac{C}{A}\right)$. With the location of maximum pin force, we can substitute into the original $F_{P(L)}$ equation to obtain equation 75.

$$F_{P(L),max} = M \cdot \frac{\left(\left(\frac{C}{A}\right)\left(\mu+\sqrt{\mu^2+1}\right)\right)-\mu\left(\frac{C}{A}\right)}{\left(\frac{C}{A}\right)^2+\left(\left(\frac{C}{A}\right)\left(\mu+\sqrt{\mu^2+1}\right)\right)^2} \tag{75}$$

The final equation for maximum pin force applied to the die tooling for linear geometry:

$$F_{P(L),max} = M\left(\frac{A}{2C}\right)\left(\frac{1}{\sqrt{\mu^2+1}+\mu}\right) \tag{76}$$

Appendix II. Moment Calculations for Female Die

Table 8. Moment summary for contact point 1

	Contact point 1						
	Layer 1	Layer 2	Layer 3	Layer 4	Layer 5	Layer 6	Layer 7
Lw (in.)	1	1	1	1	1	1	1
Lh (in.)	0.5	1	1.5	2	2.5	3	3.5
D (in.)	0	0.086	0.631	0.882	1.023	1.113	1.174
Fs (lb)	1023.7	1049.6	1235.1	1327.7	1378.2	1408.2	1427.3
Fc (lb)	409.5	434.8	661.0	820.5	933.1	1015.0	1076.6
M (lb in.)	102.4	614.8	1191.6	1834.8	2512.4	3209.6	3918.8

Table 9. Moment summary for contact point 2

	Contact point 2			
	Layer 4	Layer 5	Layer 6	Layer 7
Lw (in.)	0.75	1.25	4.75	4.75
Lh (in.)	0.5	1	1.5	2
D (in.)	0.174	0.287	0	0
Fs (lb)	3293.5	3709.1	2794.1	2794.1
Fc (lb)	997.2	1301.1	698.5	698.5
M (lb in.)	898.9	2082.8	873.2	2270.2

Table 10. Moment summary for contact point 3

	Contact point 3			
	Layer 4	Layer 5	Layer 6	Layer 7
Lw (in.)	0.375	0.500	3.500	3.500
Lh (in.)	0.5	1	1.5	2
D (in.)	0	0	0	0
Fs (lb)	1023.7	1023.7	1023.7	1023.7
Fc (lb)	1484.4	1484.4	1484.4	1484.4
M (lb in.)	-44.8	281.5	-3659.8	-3147.9

Table 11. Moment summary for contact point 4

	Contact point 4						
	Layer 1	**Layer 2**	**Layer 3**	**Layer 4**	**Layer 5**	**Layer 6**	**Layer 7**
Lw (in.)	1	1	1	1	1	1	1
Lh (in.)	0.5	1	1.5	2	2.5	3	3.5
D (in.)	0.125	0.125	0.125	0.125	0.125	0.125	0.125
Fs (lb)	2417.5	2417.5	2417.5	2417.5	2417.5	2417.5	2417.5
Fc (lb)	1607.4	1607.4	1607.4	1607.4	1607.4	1607.4	1607.4
M (lb in.)	-398.7	810.1	2018.8	3227.5	4436.3	5645.0	6853.7

Appendix III. Bolt Locations for Female Die

Table 12. Female bolt coordinates (layers 1-4)

		RADIUS	X	Y
Layer 1	C1	0.339	0.661000	4.000000
	C4	0.339	7.339000	4.000000
Layer 2	C1	0.339	0.861000	2.136720
		0.339	0.861000	4.273430
	C4	0.339	7.283060	2.167120
		0.339	7.283060	4.334240
		0.339	7.283060	6.167120
Layer 3	C1	0.339	1.061000	1.863290
		0.339	1.061000	2.931650
		0.339	1.061000	4.000000
		0.339	1.061000	6.000000
	C4	0.339	7.127350	1.000000
		0.339	7.127350	2.500000
		0.339	7.127350	4.000000
		0.339	7.127350	4.933180
		0.339	7.127350	5.866360
		0.339	7.127350	6.933180
Layer 4	C1	0.339	1.261000	1.589860
		0.339	1.261000	3.726570
		0.339	1.261000	5.726570
		0.339	1.261000	6.863280
	C2	0.339	3.489000	1.000000
		0.339	3.489000	2.000000
		0.339	3.489000	3.000000
		0.339	3.489000	4.000000
		0.339	3.489000	5.000000
		0.339	3.489000	6.000000
	C4	0.339	6.837020	0.825396
		0.339	6.837020	1.369050
		0.339	6.837020	1.912700
		0.339	6.837020	2.869050
		0.339	6.837020	3.825400
		0.339	6.837020	4.466590
		0.339	6.837020	5.107780
		0.339	6.837020	6.040960
		0.339	6.837020	7.107780

Table 13. Female bolt coordinates (layers 5-7)

		RADIUS	X	Y
Layer 5	C1	0.339	1.461000	1.000000
		0.339	1.461000	2.000000
		0.339	1.461000	3.000000
		0.339	1.461000	4.000000
		0.339	1.461000	6.000000
	C2	0.339	3.464000	0.662092
		0.339	3.464000	1.662090
		0.339	3.464000	2.662090
		0.339	3.464000	3.662090
		0.339	3.464000	4.662090
		0.339	3.464000	5.662090
		0.339	3.464000	6.337910
		0.339	3.464000	6.831040
		0.339	3.464000	7.415520
	C4	0.339	6.336030	0.500000
		0.339	6.336030	1.000000
		0.339	6.336030	2.000000
		0.339	6.336030	3.000000
		0.339	6.336030	4.000000
		0.339	6.336030	5.000000
		0.339	6.336030	6.000000
		0.339	6.336030	7.000000
Layer 6	C1	0.339	7.661000	2.000000
		0.339	7.661000	4.000000
	C4	0.339	0.339000	2.000000
		0.339	0.339000	4.000000
Layer 7	C1	0.339	7.661000	2.169500
		0.339	7.661000	4.339000
	C4	0.339	0.339000	1.661000
		0.339	0.339000	3.661000
		0.339	0.339000	5.830500

Appendix IV. Pin Locations for Female Die

Table 14. Female pin coordinates (layers 1-7)

		RADIUS	X	Y
Layer 1	C1	0.1875	0.3390	2.0000
		0.1875	7.6610	6.0000
	C4	0.1875	7.3419	1.8333
		0.1875	0.6610	6.0000
Layer 2	C1	0.1875	0.8610	1.7977
		0.1875	0.3390	6.0000
	C4	0.1875	7.6610	2.0000
		0.1875	7.2831	5.5656
Layer 3	C1	0.1875	0.3390	2.0000
		0.1875	1.0610	6.3390
	C4	0.1875	7.1306	1.7432
		0.1875	7.6610	6.0000
Layer 4	C1	0.1875	0.3390	1.0000
		0.1875	1.2610	7.5000
	C2/C3	0.1875	3.5656	0.3390
		0.1875	3.5517	1.3346
		0.1875	3.5517	2.3346
		0.1875	3.5517	3.3346
		0.1875	3.5517	4.3346
		0.1875	3.6610	5.3864
		0.1875	3.4640	5.3231
		0.1875	3.6610	7.1398
	C4	0.1875	6.3360	2.0000
		0.1875	7.6610	5.8125
Layer 5	C1	0.1875	0.3390	3.0000
		0.1875	1.2610	6.2734
	C2/C3	0.1875	3.3390	0.3473
		0.1875	3.3390	1.3473
		0.1875	3.3390	2.3473
		0.1875	3.3390	3.3473
		0.1875	3.3390	4.3473
		0.1875	3.3390	5.1836
		0.1875	3.7037	6.5776
		0.1875	3.7037	7.6552
	C4	0.1875	7.6610	2.3390
		0.1875	4.8392	6.0000
Layer 6	Locating	0.1875	0.3390	1.0000
		0.1875	7.6610	5.8125
Layer 7	Locating	0.1875	0.3390	2.3390
		0.1875	7.6610	5.0000

Appendix V. Moment Calculations for Male Die

Table 15. Moment summary for contact point 1

	Contact point 1						
	Layer 1	Layer 2	Layer 3	Layer 4	Layer 5	Layer 6	Layer 7
Lw (in.)	1.125	1.25	4.791	4.949	5.000	6.000	6.000
Lh (in.)	0.5	1	1.5	2	2.5	3	3.5
D (in.)	0.000	0.000	0.000	0.000	0.000	0.000	0.000
Fs (lb)	1023.7	1023.7	1023.7	1023.7	1023.7	1023.7	1023.7
Fc (lb)	409.5	409.5	409.5	409.5	409.5	409.5	409.5
M (lb in.)	51.2	511.9	-426.3	20.9	511.9	614.2	1126.1

Table 16. Moment summary for contact point 2

	Contact point 2						
	Layer 1	Layer 2	Layer 3	Layer 4	Layer 5	Layer 6	Layer 7
Lw (in.)	1.2	1.4	1.6	1.8	2.0	3.0	3.0
Lh (in.)	0.5	1	1.5	2	2.5	3	3.5
D (in.)	0.000	0.220	0.3678	0.43866	0.47984	0.396447	0.45644
Fs (lb)	2794.1	3451.1	4060.9	4413.3	4636.4	4198.447	4508.09
Fc (lb)	698.5	1106.0	1605.9	1965.5	2228.4	1739.053	2073.43
M (lb in.)	558.8	1902.8	3522.0	5288.7	7134.3	7378.179	9558.02

Table 17. Moment summary for contact point 3

	Contact point 3						
	Layer 1	Layer 2	Layer 3	Layer 4	Layer 5	Layer 6	Layer 7
Lw (in.)	1.500	2.000	2.291	2.449	2.500	3.500	3.500
Lh (in.)	0.5	1	1.5	2	2.5	3	3.5
D (in.)	0	0	0	0	0	0	0
Fs (lb)	1023.7	1023.7	1023.7	1023.7	1023.7	1023.7	1023.7
Fc (lb)	1484.4	1484.4	1484.4	1484.4	1484.4	1484.4	1484.4
M (lb in.)	-1714.7	-1945.0	-1865.1	-1587.8	-1151.7	-2124.2	-1612.3

Table 18. Moment summary for contact point 4

	Contact point 4						
	Layer 1	**Layer 2**	**Layer 3**	**Layer 4**	**Layer 5**	**Layer 6**	**Layer 7**
Lw (in.)	0.5	1.0	3.1	3.3	3.5	4.5	4.5
Lh (in.)	0.5	1	1.5	2	2.5	3	3.5
D (in.)	0.125	0.125	0.125	0.125	0.125	0.125	0.125
Fs (lb)	2417.5	2417.5	2417.5	2417.5	2417.5	2417.5	2417.5
Fc (lb)	1607.4	1607.4	1607.4	1607.4	1607.4	1607.4	1607.4
M (lb in.)	405.0	810.1	-1356.7	-469.5	417.8	19.1	1227.8

Appendix VI. Bolt Locations for Male Die

Table 19. Male bolt coordinates (layers 1 – 7)

		RADIUS	X	Y
Layer 1	C2	0.339	2.661000	2.000000
		0.339	2.661000	4.000000
	C4	0.339	4.500000	4.000000
Layer 2	C2	0.339	2.786000	1.157400
		0.339	2.786000	2.314800
		0.339	2.786000	3.200000
		0.339	2.786000	4.314800
		0.339	2.786000	5.236100
		0.339	2.786000	6.157400
	C4	0.339	5.658030	4.000000
Layer 3	C2	0.339	6.250000	2.000000
		0.339	6.250000	4.000000
Layer 4	C2	0.339	6.500000	1.500000
		0.339	6.500000	4.300760
		0.339	6.500000	6.150380
Layer 5	C2	0.339	6.605060	1.961760
		0.339	6.605060	3.961760
		0.339	6.605060	5.811380
		0.339	6.605060	6.905690
Layer 6	C2	0.339	7.661000	2.000000
		0.339	7.661000	4.000000
		0.339	7.661000	6.000000
Layer 7	C2	0.339	7.661000	1.169500
		0.339	7.661000	2.500000
		0.339	7.661000	4.500000
		0.339	7.661000	6.500000

Appendix VII. Pin Locations for Male Die

Table 20. Male pin coordinates (layers 1 – 7)

		RADIUS	X	Y
Layer 1	C1/C2	0.1875	2.3390	0.5000
		0.1875	2.6610	1.5000
		0.1875	2.6610	2.6296
		0.1875	2.6610	3.6296
		0.1875	2.6610	4.6296
		0.1875	2.6610	5.5000
		0.1875	2.6610	6.5000
		0.1875	2.3390	7.5000
	C3/C4	0.1875	4.5000	1.0000
		0.1875	4.5000	3.0000
		0.1875	4.5000	5.0000
		0.1875	4.5000	6.0000
Layer 2	C1/C2	0.1875	2.7860	0.5000
		0.1875	2.1390	1.5000
		0.1875	2.1390	2.5000
		0.1875	2.1390	3.5000
		0.1875	2.1390	4.5000
		0.1875	2.1390	5.5000
		0.1875	2.1390	6.5000
		0.1875	2.7860	7.5000
	C3/C4	0.1875	4.3390	0.5000
		0.1875	5.6580	3.0000
		0.1875	5.6580	5.0000
		0.1875	4.3390	7.0000
Layer 3	C1/C4	0.1875	1.9390	1.0000
		0.1875	6.1590	3.0000
		0.1875	1.9390	5.0000
		0.1875	6.1590	7.0000
Layer 4	C1/C4	0.1875	6.4494	1.0000
		0.1875	1.7390	3.0000
		0.1875	6.4494	5.0000
		0.1875	1.7390	7.0000
Layer 5	C1/C4	0.1875	1.5390	1.0000
		0.1875	6.6051	3.1043
		0.1875	1.5390	5.0000
		0.1875	6.6051	7.5000
Layer 6	Locating	0.1875	0.3390	2.3390
		0.1875	0.3390	6.0000
Layer 7	Locating	0.1875	0.3390	5.0000
		0.1875	7.6610	3.0000